PERGAMON

International Journal of Solids and Structures 40 (2003) 181–217

INTERNATIONAL JOURNAL OF SOLIDS and STRUCTURES

www.elsevier.com/locate/ijsolstr

Rheological–dynamical analogy: modeling of fatigue behavior

Dragan D. Milašinović *

Department of Civil Engineering, University of Novi Sad, Kozaračka 2a, 24000 Subotica, Yugoslavia

Received 11 June 2001; received in revised form 15 August 2002

Abstract

Present paper relates to the analysis of fatigue and fatigue failure of thin long steel bars with the application of a new rheological model and rheological–dynamical analogy (RDA). The analogy has been developed on the basis of mathematical–physical analogy between rheological model and dynamical model with viscous damping, and is aimed to be used for the analysis of inelastic deforming of materials and structures. In this presentation, the aim will be to highlight different aspects of fatigue behavior and fill the gap that other methods cannot. This paper provides a numerical example of obtaining *S–N* curves of thin long steel bars using RDA model and description of the hysteretic energy dissipation of material subjected to cyclic stresses. First the axial fatigue setup and the experimental results are discussed. The latter in order to demonstrate the ability of the RDA modeling technique, the comparison with Griffith's theory of fracture is presented. RDA method for fatigue crack growth rate is proposed and compared with Paris power law. On the basis of the comparisons, the present RDA method could be considered as valid and suitable for modeling of fatigue behavior.
© 2002 Elsevier Science Ltd. All rights reserved.

Keywords: New rheological model; Rheological–dynamical analogy; RDA *S–N* curves; RDA rate of release of potential energy; RDA fatigue crack growth rate

1. Introduction

The failure of materials under a variable load at stresses lower than the ultimate strength is called fatigue failure. This name does not reflect the physical nature of the phenomenon, but it has become such a customary term that it is used to this day.

Experiments show that under alternative tension or compression a decrease in the acting force results in an increase in the number of alterations of this force required breaking the specimen. Each material has a maximum normal stress at which the specimen can withstand practically unlimited number of alterations of the force without breaking down. This stress is denoted by σ_e (stress when the fatigue crack appears) and is called the fatigue limit or the endurance limit.

* Tel.: +381-24-554-300; fax: +381-24-554-580/23-022.
E-mail address: ddmil@gf.su.ac.yu (D.D. Milašinović).

0020-7683/02/$ - see front matter © 2002 Elsevier Science Ltd. All rights reserved.
PII: S0020-7683(02)00518-8

Nomenclature

a	crack length
a_0, a_1, a_2	material constants
A, A_1, A_2	cross-sectional area of the bar
A_{red}	reduced cross-sectional area of the bar
A_{s}	fracture area or crack area
A^*	unit cross-sectional area
A, B, C	constant of integration
b	sample width
c	phase velocity of mechanical wave
c, c_{c}	viscous damping, critical damping
C	axis intercept
$\mathrm{d}a/\mathrm{d}N_{\mathrm{c}}$	rate of crack growth
$\mathrm{d}\varepsilon^{\mathrm{H}}$	infinitesimal extension
$\mathrm{d}l$	infinitesimal change of the length
E_{H}	slope of the elastic strain or Young's modulus
E_{K}	slope of the viscoelastic strain or viscoelastic modulus
$E_{\mathrm{K}}^{\mathrm{D}}$	dynamic viscoelastic modulus
f	frequency of external force
f_σ	frequency of a variable stress cycle
F	geometric factor
g	gravity acceleration
G_{I}, G_{I}^*	Griffith's rate of release of potential energy
$G_{\mathrm{I,c}}$	RDA rate of release of potential energy
$\mathbf{H}$	symbol for the Hooken spring
H'	slope of the viscoplastic strain or viscoplastic modulus
H'^{D}	dynamic viscoplastic modulus
I_z	moment of inertia (of cross-section)
k	stiffness
k_z	radius of gyration
$\mathbf{K}$	symbol for the Kelvin's body: $\mathbf{K} = \mathbf{H}\|\mathbf{N}$
K_{I}, K_{I}^*	stress intensity factor
$K_{\mathrm{I,c}}$	RDA stress intensity factor
$K_{\max}$	maximum absolute stress intensity factor
$K_{\min}$	minimum absolute stress intensity factor
l_0	unstretched length of the bar
l_{p}	length of the bar for slenderness ratio on proportional limit
m	mass
m	slope of crack growth curve
$\mathbf{N}$	symbol for the Newtonian dashpot
N	number of cycles in the loading time
N_{e}	number of cycles for fatigue life
N_{c}	number of cycles for fatigue failure life
P	compression external force
P_σ	constant of integration

Q	heat or thermal energy
Q_σ	constant of integration
r	coefficient of asymmetry of cycle
R	RDA dimensional parameter
S, S_1, S_2	tension external force
StV	symbol for the Saint-Venant's body
t	time
t_0	initial instant of time
t_c	fatigue failure life
t_e	fatigue life
t_p	time when proportional stress has been achieved
$t - t_0$	time difference
T^*	time of retardation in the viscoplastic yielding
T_K	time of retardation
T_K^D	dynamic time of retardation
u	displacement of the particles
U_1, U_e	elastic potential energy
U_d	hysteretic energy dissipation
U_s	energy to produce a unit area of fracture surface
U_T	total mechanical energy
$U_2 - U_1$	change in internal energy
v, v_1, v_2	velocity of the particles
W	potential energy of the external forces
$W_{d,el}$	rate of release of elastic energy
$W_{d,ve}$	rate of release of viscoelastic energy
W_T	thermal expansion work
Y	stress level for viscoplastic yielding
α	phase angle
α_T	coefficient of linear thermal expansion
γ	specific gravity
γ_s	specific surface energy
δ	ratio of load frequency to the frequency of natural vibrations or relative frequency
δ_1	relative frequency for first cycle
δ_c	relative frequency for fatigue failure life
δ_e	relative frequency for fatigue life
$\Delta G_{I,c}$	RDA rate of release of potential energy range
ΔK	stress intensity range
$\Delta K_{I,c}$	RDA stress intensity range
Δl, Δl_1, Δl_2	increase in length
ΔT, ΔT_{ve}, ΔT_{el}	difference between the final temperature and the original temperature
$\Delta\sigma$	stress range
ε	total inelastic strain
ε_l	axial strain
ε_t	lateral strain
ε^H	Hencky's measure of extension
$\dot{\varepsilon}$, $\dot{\varepsilon}_1$, $\dot{\varepsilon}_2$	strain rate

$\ddot{\varepsilon}$	strain acceleration
ε_{h}	complementary strain
ε_{p}	particular strain
$\dot{\varepsilon}_{\mathrm{p}}$	particular strain rate
ε'	strain due constant stress
ε^{c}	creep strain
$\varepsilon''_{\mathrm{p}}$	strain vary periodically or sinusoidal with time
ε_{A}	cyclic strain amplitude
$\varepsilon_{\mathrm{el}}$	elastic strain
$\varepsilon_{\mathrm{ve}}$	viscoelastic strain
$\dot{\varepsilon}_{\mathrm{ve}}$	viscoelastic strain rate
$\varepsilon_{\mathrm{vp}}$	viscoplastic strain
$\dot{\varepsilon}_{\mathrm{vp}}$	viscoplastic strain rate
η	RDA dynamical coefficient
λ_{K}	viscoelastic coefficient of normal viscosity (Trouton's coefficient)
λ_{N}	viscoplastic coefficient of normal viscosity (Trouton's coefficient)
λ_{P}	slenderness ratio on proportional limit
μ	Poisson's ratio
μ^{H}	Poisson's ratio for the Hencky's measure of extension
Π	total potential energy
ρ	mass density
σ, σ_1, σ_2	variable stress
$\dot{\sigma}$	stress rate
$\ddot{\sigma}$	stress acceleration
σ_0	constant stress or mean cycle stress
σ''	stress vary periodically or sinusoidal with time
σ_{A}	amplitude of stress
σ_{p}	proportional stress
σ_{p}^{E}	Euler's proportional stress
$\sigma_{\mathrm{p}}^{\mathrm{RDA}}$	RDA proportional stress
σ_{cr}	critical stress
σ_{SV}	stress in the Saint-Venant's element
σ_{Y}	uniaxial yield stress
$\sigma_{\max}$	maximum absolute stress in the cycle
$\sigma_{\min}$	minimum absolute stress in the cycle
$\sigma_{\max,\mathrm{c}}$	maximum applied dynamical stress
σ_{e}	fatigue limit
σ_{N}	nominal stress at the crack
σ_{c}	RDA fracture stress
φ	creep coefficient
φ^*	structural creep coefficient
Φ, Φ_1, Φ_2	diameter of the bar
Φ_{red}	reduced diameter of the bar
ω	circular natural frequency
ω_σ	stress circular frequency

|	symbol for parallel connection
—	symbol for serial connection
H–K–(N|StV)	symbol for a new rheological model

The physical phenomenon of fatigue was first seriously considered in the mid-nineteenth century when widespread failures of railway axles in Europe prompted Wöhler (1867) in Germany and Fairbairn in England to conduct the first systematic investigations into the fracture of materials under cyclic stresses around 1860.

However, the main impetus for research directed at the crack propagation stage of fatigue failure, as opposed to mere lifetime calculations, did not occur until the mid-1960s when the concepts of linear elastic fracture mechanics (LEFM) and so-called "defect-tolerant design" were first applied to the problem of subcritical flaw growth. Griffith (1921, 1925) used the solution of Inglish (1913) to determine the rate of release of potential energy. Orowan (1948) and Irwin (1948) saw that a plastic zone forms at the tip of a crack in high strength metals and, provided this zone is small, the plastic work required to create a unit area of fracture surface is a material constant that can be added to the surface energy. Crack surface opened under load and Wells (1961) suggested that in metals, fracture occurs when the crack tip opening displacement reaches a critical value. The concept is most readily applied in conjunction with the fictitious crack model of Hillerborg et al. (1976). Although he did not call it a fictitious crack, the concept was first applied by Dugdale (1960) to the problem of a Griffith crack in an elasto-plastic solid.

This approach recognizes that all structures are flawed, and that cracks may initiate early in service life and propagate subcritically. Lifetime is then assessed on the basis of the time or the number of loading cycles for the largest undetected crack to grow to failure, as might be defined by an allowable strain, or limit load or fracture toughness (K_{Ic}) criterion. Implicit in such analyses is that sub critical crack growth can be characterized in terms of some governing parameter (often thought of as an effective "crack driving force") which describes local conditions at the crack tip yet may be determined in terms of loading parameters, crack size and geometry. Linear elastic and elastic–plastic fracture mechanics have, to date, provided the most appropriate methodology for such analyses to be made, and consequently, considerable effort has been directed towards defining parameters which uniquely stress and strain fields at the crack tip over length scales characteristic of the local fracture mechanisms involved.

The concept of directly applying fracture mechanics to subcritical fatigue crack growth was first suggested by Paris et al. (1961) in their famous "Rational Analytic Theory of Fatigue". Despite difficulties in finding the physical nature of the phenomenon, their proposal of correlating fatigue crack propagation rates (da/dN) with the stress intensity factor (K_I) has remained the basis of the defect-tolerant fatigue design approach ever since. The rate of growth of a crack caused by fatigue loading is approximately given by Paris law (Paris and Erdogan, 1963). This law has found wide applicability for fatigue growth of cracks in metals.

Based on the concept that crack tip stress and deformation fields in an elastic–plastic strain hardening solid can be described by the Hutchinson–Rice–Rosengren (Rice and Rosengren, 1968) singularity and thus uniquely characterized by the J-integral, Dowling (1976) suggested that fatigue crack propagation in the presence of extensive plasticity could be correlated to the range of J, that is, ΔJ, which under linear-elastic conditions would be equal to $\Delta K^2/E$, where ΔK is stress intensity range.

Although fatigue represents one of the major causes of failure in engineering service, a complete understanding the mechanical fatigue due to cyclic stress has not yet been reached. Good progress might be made by using rheological–dynamical analogy (RDA). In the course of my research work I developed a new model of viscoelasto-plastic material that is able to describe the mutual interaction of elasticity, viscoelasticity and viscoplasticity. Based on this model, the RDA is established as the theoretical concept for studying the inelastic material deforming. This analytical concept has been already used and proved

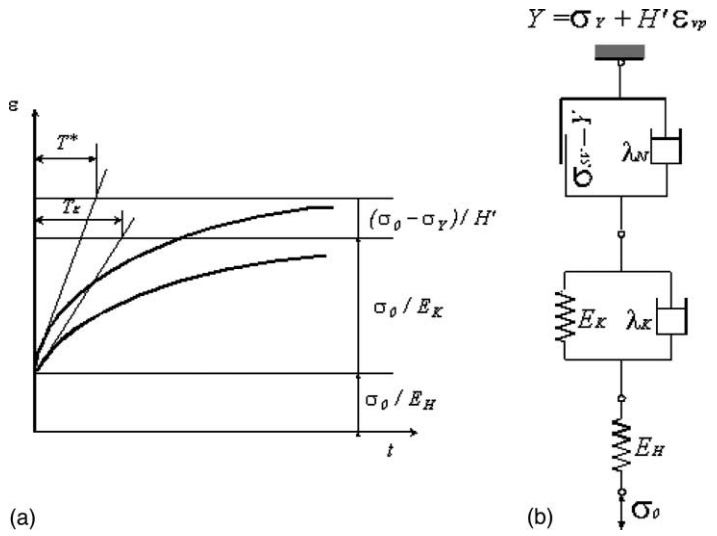

Fig. 1. (a) Change of strain according to the proposed model. (b) A new rheological model of viscoelasto-plastic body.

through several inelastic problems (Milašinović, 1996, 1997, 2000). The employed RDA is based on a new rheological model, H–K–(N|StV), of viscoelasto-plastic material, and mathematical–physical analogy between rheological model and dynamical model with viscous damping. It occurs only when there is the arrangement of five fundamental elements making up the body as shown in Fig. 1b. The parameter H' (the slope of the viscoplastic strain), furthermore, must be included in the yield condition. All of the other previously mentioned combinations with less or more fundamental elements could not restore this analogy. Furthermore when dealing with development of the mathematical–physical models for fatigue behavior the main advantages of the RDA formulation are associated with its simple and rigorous mathematical–physical structure allowing for analytical solutions.

The objective of the present paper is to explain the physical mechanism and to find the experimental proof for the new rheological model and RDA. Theoretical consideration has also been made to confirm the applicability of RDA method that other methods cannot. The present paper presents newly developed *S–N* curves from relationships such as the RDA describes the form of the constant amplitude. Closed form analytical solutions for the rate of release of viscoelastic energy were derived as well as the fatigue life, the fatigue failure life, and the change in the temperature of the body. Furthermore, Bernoulli's energy theorem is used for the evaluation of the localized reduction of cross-section area, from which we obtain: the fracture stress, the maximum applied dynamical stress, the rate of release of potential energy, and fatigue crack growth rate.

For a more exact elucidation of the RDA, this author is introduced RDA prediction to simulate experimental results of the increased temperature of the specimen under axial fatigue, including distinction between viscoelastic and elastic behavior.

Due to the present observation, fundamentally new, our understanding of fatigue behavior can be achieved.

2. A new rheological model

The results of experimental research of strains show that their development and magnitude are dependent on time, and because of that the rheological analysis proves unavoidable. Elasticity, plasticity, viscosity and

strength are essential rheological properties from which most of other complex properties may be derived (Reiner, 1955). The ideal bodies, typifying the three fundamental properties of elasticity, plasticity and viscosity, can be conveniently represented by the following rheological models (Hookean spring, Saint-Venant's resistance and Newton's dashpot). Combining the rheological elements, various structural rheological models illustrating the stress–strain relationships of technical media can be obtained.

As stated earlier, the majority of materials are in the state of elasticity and viscoelasticity in the conditions of low loading, whereas after reaching the yield stress, it transits to the state of viscoplasticity. Every strain is in principle a function of time because a stress is always introduced into the body during a definite time interval (even a very small one) and therefore the distinction between a time-dependent strain and a strain not depending on time is very uncertain. Here, it is assumed that the strain is measured when the specified stress has been reached. Strain ε_{el} obtained in this way shall be considered to be independent of time, i.e. instantaneous. Then the time-dependent, or delayed, ε_{ve} and ε_{vp} strains are measured from the time, when the instantaneous strain has developed. Elastic material behavior can be modeled by a linear spring (**H**). Therefore, instantaneous or initial strain should be $\varepsilon_{el} = \sigma_0/E_H$ where E_H is the elastic modulus. Delayed elastic or viscoelastic strain ε_{ve} may be imagined as a common behavior of elastic E_K and viscous λ_K materials. A piston exerting pressure on a liquid with a viscosity λ_K represents ideal viscous material. Viscoelastic material behavior can be modeled by Kelvin's model (**K**), where the elastic and viscous elements are linked in parallel. The concept of delayed plastic or viscoplastic material behavior ε_{vp} may be imagined as a common behavior of the friction slider component σ_{SV} and viscous component λ_N of materials. The friction slider develops a stress σ_{SV}, becoming active only if $\sigma \geqslant Y = \sigma_Y + H'\varepsilon_{vp}(t)$, where σ is the total applied stress and Y is some limiting yield value. The stress level in the friction slider depends on whether the threshold or yield stress Y, has been reached. If the stress σ is discontinued, the friction slider does not return into its original position. Viscoplastic material behavior can be modeled by the third of the sequentially linked models (**N|StV**) as shown in Fig. 1b. Initial strain rate should be $\dot{\varepsilon} = \sigma_0/\lambda_K + (\sigma - \sigma_0)/\lambda_N$.

Summarizing the above-mentioned assumptions, a new rheological model may be presented by the following structural equation:

$$\mathbf{H}\text{–}\mathbf{K}\text{–}(\mathbf{N}|\mathbf{StV}). \tag{1}$$

The corresponding differential equation (Milašinović, 2000) is

$$\ddot{\varepsilon}(t) + \dot{\varepsilon}(t)\left(\frac{E_K}{\lambda_K} + \frac{H'}{\lambda_N}\right) + \varepsilon(t)\frac{E_K H'}{\lambda_K \lambda_N} = \frac{\ddot{\sigma}(t)}{E_H} + \dot{\sigma}(t)\left(\frac{E_K}{\lambda_K E_H} + \frac{H'}{\lambda_N E_H} + \frac{1}{\lambda_K} + \frac{1}{\lambda_N}\right) + \sigma(t)\left(\frac{E_K}{\lambda_K \lambda_N} + \frac{H'}{\lambda_K \lambda_N} + \frac{E_K H'}{\lambda_K \lambda_N E_H}\right) - \sigma_Y \frac{E_K}{\lambda_K \lambda_N}. \tag{2}$$

The homogeneous equation of the inhomogeneous equation (2) has the following form

$$\ddot{\varepsilon}(t)\lambda_K \lambda_N + \dot{\varepsilon}(t)(E_K \lambda_N + H'\lambda_K) + \varepsilon(t)E_K H' = 0, \tag{3}$$

where λ_K, λ_N, E_K and H' are given constants at fixed step time.

3. Physical mechanism of the rheological–dynamical analogy

3.1. A mechanical waves

Of the different ways in which energy can be transferred, the wave-transfer mechanism is unique in that energy is transmitted without the physical transfer of material from the source. A mechanical wave is a

disturbance that moves through mater. To produce mechanical waves, we need a source of energy which produces a disturbance, and an elastic medium to transmit the disturbance. The elastic medium obeys Hooke's law. The propagation of waves in a uniform isotropic medium can be described by a partial differential equation, called the wave equation (Timoshenko and Goodier, 1951). Thus

$$\frac{\partial^2 u}{\partial t^2} = c^2\left(\frac{\partial^2 u}{\partial x^2} + \frac{\partial^2 u}{\partial y^2} + \frac{\partial^2 u}{\partial z^2}\right). \tag{4}$$

Let us imagine a thin long symmetrical bar (say, with a square or circular cross-section), with the length l_0 and the circular cross-sectional area A. Then the wave equation may be represented in the following form

$$\frac{\partial^2 u}{\partial t^2} = c^2\frac{\partial^2 u}{\partial x^2}. \tag{5}$$

Here u is displacement of the particles. The propagation of longitudinal waves in a thin long bar is associated with its longitudinal tension and compression. Hence, the phase velocity of such waves is

$$c = \sqrt{\frac{E_{\mathrm{H}}}{\rho}}, \tag{6}$$

where ρ is the density of the undisturbed medium.

The velocity of the particles is

$$v = c\varepsilon_{\mathrm{el}} = \frac{\sigma}{\sqrt{E_{\mathrm{H}}\rho}}, \tag{7}$$

where $\sigma = S/A$ is stress or the ratio of the internal force, S to the cross-section area, A, and $\varepsilon_{\mathrm{el}} = \Delta l/l_0$ is elastic strain (elongation) or the ratio of the increase in length, Δl to the unstretched length, l_0.

The maximum displacement of the vibrating particles of the medium is the amplitude of the wave motion. It is determined by the energy of the wave. In practical system, wave energy is dissipated and the wave amplitude gradually diminishes. The reduction in amplitude of a wave due to the dissipation of wave energy as it travels away from the source is called damping.

3.2. Rheological–dynamical analogy

However, from a new rheological model input parameters listed, only E_{H} is relatively easy to measure experimentally. To apply the model to real materials, we need to relate the remaining parameters to physically an alternative means by virtue of their mathematical descriptions. We shall now consider the problem in which the applied forces vary with time so that dynamic stresses are setup in the body.

A mechanical disturbance (strain) propagates in an elastic medium at the finite velocity c. Therefore, strains, initiated by the wave source at the instant t_0 of time, reach an arbitrary point M of the bar at the instant $t > t_0$. The greater the path l the wave travels from its source to point M, for the greater the difference $t - t_0 = l/c$. Consequently, the vibration at point M lags in phase behind that at the source of the waves. If l_0 is the distance between two ends of the bar the difference $t - t_0$ is

$$T_{\mathrm{K}}^{\mathrm{D}} = t - t_0 = \frac{l_0}{c}. \tag{8}$$

Under tension and compression of the bar, the frequency of natural vibrations is

$$\omega = \sqrt{\frac{k}{m}} = \sqrt{\frac{E_{\mathrm{H}}A}{l_0}\frac{1}{\rho A l_0}} = \sqrt{\frac{E_{\mathrm{H}}}{\rho}}\frac{1}{l_0} = \frac{c}{l_0} = \frac{1}{T_{\mathrm{K}}^{\mathrm{D}}}. \tag{9}$$

Initial strain rate, according to the proposed rheological model is

$$\dot{\varepsilon} = \dot{\varepsilon}_{ve} + \dot{\varepsilon}_{vp} = \sigma_0/\lambda_K + (\sigma - \sigma_0)/\lambda_N, \tag{10}$$

while from diagram in Fig. 1a is

$$\dot{\varepsilon}_{ve} + \dot{\varepsilon}_{vp} = [\sigma_0/E_K + (\sigma_0 - \sigma_Y)/H']/T^*. \tag{11}$$

Comparing above equations, we obtain

$$\sigma_0/\lambda_K + (\sigma_0 - \sigma_Y)/\lambda_N = [\sigma_0/E_K + (\sigma_0 - \sigma_Y)/H']/T^*, \tag{12}$$

so that

$$\lambda_N = (\sigma_0 - \sigma_Y)/\{[\sigma_0/E_K + (\sigma_0 - \sigma_Y)/H']/T^* - \sigma_0/\lambda_K\}. \tag{13}$$

The strain rates $\sigma_0/(E_K T^*)$ and σ_0/λ_K are very small values in comparison with the rate in the viscoplastic yielding $(\sigma_0 - \sigma_Y)/(H'T^*)$. Therefore, they can be neglected without an influence on the result. Because of that, the coefficient of viscosity can be taken as

$$\lambda_N = H'T^*. \tag{14}$$

According to the Kelvin's body there is

$$\lambda_K = E_K T_K, \tag{15}$$

where T_K represents the time of retardation.

Heaving in mind Eq. (3), we can formulate expression similar to formula (9), turning the model into the case of critical damping, $E_K/\lambda_K = H'/\lambda_N$ (Milašinović, 2000)

$$\sqrt{\frac{E_K H'}{\lambda_K \lambda_N}} = \sqrt{\frac{1}{T_K T^*}} = \frac{1}{T_K^D}, \tag{16}$$

where T_K^D represents the dynamical time of retardation.

According to formulas (9) and (16) we shall have:

$$\sqrt{\frac{E_H}{\rho}}\frac{1}{l_0} = \sqrt{\frac{E_K H'}{\lambda_K \lambda_N}} \Rightarrow \lambda_K \lambda_N = \frac{E_K H' \gamma l_0^2}{E_H g} \Rightarrow \frac{\lambda_K \lambda_N}{\gamma} = \frac{E_K H' A l_0^2 \rho}{E_H \gamma A} = \frac{E_K H'}{\gamma k} m, \tag{17}$$

where

$$m = \frac{\lambda_K \lambda_N}{\gamma}, \quad k = \frac{E_K H'}{\gamma}. \tag{18}$$

Critical damping is

$$c = c_c = 2\sqrt{km} = 2\frac{E_K \lambda_N}{\gamma}. \tag{19}$$

By these assumptions, we turned one very complicate nonlinear viscoelasto-plastic problem into a simpler linear dynamical one.

Replacing $\lambda_K \lambda_N$ by $m\gamma$, $E_K \lambda_N + H' \lambda_K$ by $c\gamma$ and $E_K H'$ by $k\gamma$, the differential equation (3) becomes

$$\ddot{\varepsilon}(t)m + \dot{\varepsilon}(t)c + \varepsilon(t)k = 0, \tag{20}$$

where

$$m = \frac{\lambda_K \lambda_N}{\gamma}, \quad c = \frac{(E_K \lambda_N + H' \lambda_K)}{\gamma}, \quad k = \frac{E_K H'}{\gamma}. \tag{21}$$

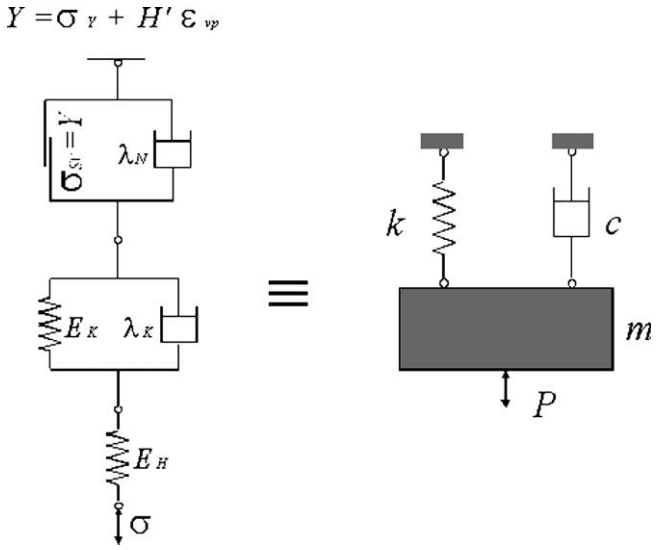

Fig. 2. Analogy between a new rheological model and dynamical model with viscous damping.

Analogy between differential equation (20) and differential equation of damped free vibration of single-degree-of-freedom (SDOF) system becomes obvious. Coefficients are dimensionally equal in these equations. Therefore, a very important new mathematical–physical analogy between the new rheological model and the dynamical model with viscous damping, Fig. 2, can be formulated. In accordance with this it is obvious that inelastic response of engineering structures is essentially a dynamical problem. The rheology is a branch of physics, which is closest to mechanics. The analogy exists for a very specific rheological model, and is one example of numerous analogies that can be observed in mechanics, as well as between mechanical and electrical (thermal, magnetic, etc.) systems, by virtue of their mathematical descriptions.

4. Cyclic stresses

4.1. Coefficient of asymmetry of cycle

From among the various types of steady variable stresses, cyclic stresses are the most important; besides, these stresses are the most widely investigated. The curves, which describe the variation of stresses in time, may considerably differ in appearance; variation of stresses in machine parts often follows the sinusoidal law

$$\sigma(t) = \sigma_0 + \sigma_A \sin(\omega_\sigma t), \tag{22}$$

where ω_σ = load or stress frequency.

The maximum absolute stress in the cycle is denoted by σ_{max}, while the minimum is denoted by σ_{min}. The ratio of minimum stress to maximum with the signs taken into account is known as the cycle characteristic, or the coefficient of asymmetry of cycle

$$r = \frac{\sigma_{min}}{\sigma_{max}}. \tag{23}$$

The coefficient varies between -1 and $+1$. The half of the sum of maximum and minimum stresses of a cycle (taking into consideration their signs) is known as the constant component of cycle, or mean cycle stress.

$$\sigma_0 = \frac{\sigma_{\max} + \sigma_{\min}}{2} = \frac{1+r}{2}\sigma_{\max}. \tag{24}$$

The half of the difference of maximum and minimum stresses (also taking into consideration their signs) is known as the variable component of cycle or the amplitude of stresses in the cycle

$$\sigma_A = \frac{\sigma_{\max} - \sigma_{\min}}{2} = \frac{1-r}{2}\sigma_{\max}. \tag{25}$$

4.2. Dynamic coefficient using RDA

The RDA equation due to sinusoidal stresses takes the form of:

$$\ddot{\varepsilon}(t)m + \dot{\varepsilon}(t)c + \varepsilon(t)k = \sigma_A\left(\frac{k}{E_H} + \frac{E_K + H'}{\gamma} - \omega_\sigma^2\frac{m}{E_H}\right)\sin(\omega_\sigma t) + \sigma_A\left(\frac{c}{E_H} + \frac{\lambda_K + \lambda_N}{\gamma}\right)\omega_\sigma\cos(\omega_\sigma t) + \sigma_0\left(\frac{k}{E_H} + \frac{E_K + H'}{\gamma}\right) - \sigma_Y\frac{E_K}{\gamma}. \tag{26}$$

The solution for this second order differential equation with constant coefficients is

$$\varepsilon(t) = \varepsilon_h + \varepsilon_p, \tag{27}$$

where ε_h is the complementary solution and ε_p is the particular solution for the given equation:

$$\varepsilon_p = A\sin(\omega_\sigma t) + B\cos(\omega_\sigma t) + C, \tag{28}$$

where A, B and C are constants:

$$A = \frac{P_\sigma(k - m\omega_\sigma^2) + Q_\sigma c\omega_\sigma}{(k - m\omega_\sigma^2)^2 + (c\omega_\sigma)^2}, \quad B = \frac{Q_\sigma(k - m\omega_\sigma^2) - P_\sigma c\omega_\sigma}{(k - m\omega_\sigma^2)^2 + (c\omega_\sigma)^2}, \quad C = \sigma_0\left(\frac{1}{E_H} + \frac{1}{E_K} + \frac{1}{H'}\right) - \sigma_Y\frac{1}{H'}, \tag{29}$$

and

$$P_\sigma = \sigma_A\left(\frac{k}{E_H} + \frac{E_K + H'}{\gamma}\right) - \sigma_A\omega_\sigma^2\frac{m}{E_H}, \quad Q_\sigma = \sigma_A\left(\frac{c}{E_H} + \frac{\lambda_K + \lambda_N}{\gamma}\right)\omega_\sigma. \tag{30}$$

Strain under constant stress, taking into consideration delayed elastic or viscoelastic strain is

$$\varepsilon'(t) = \varepsilon_h + C = \varepsilon^c = \frac{\sigma_0}{E_H} + \frac{\sigma_0}{E_K}\left(1 - e^{-(t/T_K)}\right) = \frac{\sigma_0}{E_H(t_0)}(1 + \varphi), \tag{31}$$

where creep coefficient is

$$\varphi(t) = \frac{\varepsilon_{ve}}{\varepsilon_{el}} = \frac{E_H(t_0)}{E_K}\left(1 - e^{-(t/T_K)}\right). \tag{32}$$

Cyclic strain is given by

$$\varepsilon_p''(t) = A\sin(\omega_\sigma t) + B\cos(\omega_\sigma t), \tag{33}$$

or

$$\varepsilon_p''(t) = \varepsilon_A\sin(\omega_\sigma t - \alpha), \tag{34}$$

where cyclic strain amplitude and phase difference by which the strain lags behind the stress are:

$$\varepsilon_A = \sqrt{\frac{P_\sigma^2 + Q_\sigma^2}{(k - m\omega_\sigma^2)^2 + (c\omega_\sigma)^2}}, \quad \tan\alpha = \frac{P_\sigma c\omega_\sigma - Q_\sigma(k - m\omega_\sigma^2)}{P_\sigma(k - m\omega_\sigma^2) + Q_\sigma c\omega_\sigma}. \tag{35}$$

When the structural member is loaded cyclically, the rheological behavior of the member must be characterized by the dynamic time of retardation $T_{\mathrm{K}}^{\mathrm{D}}$. Now, taking into account formula (32) we have RDA viscoelastic modulus

$$E_{\mathrm{K}}^{\mathrm{D}}(t,t_0)=\frac{E_{\mathrm{H}}(t_0)}{\varphi(t)}\left(1-\mathrm{e}^{-(t/T_{\mathrm{K}}^{\mathrm{D}})}\right)=\frac{E_{\mathrm{H}}(t_0)}{\varphi(t)}, \tag{36}$$

where

$$\mathrm{e}^{-(t/T_{\mathrm{K}}^{\mathrm{D}})}\approx 0. \tag{37}$$

Taking into consideration formula (36), we find the following expression for cyclic strain amplitude and phase or loss angle

$$\varepsilon_{\mathrm{A}}=\frac{\sigma_{\mathrm{A}}}{E_{\mathrm{H}}(t_0)}\sqrt{\frac{(1+\varphi)^2+\delta^2}{1+\delta^2}},\quad \tan\alpha=\frac{\delta\varphi}{1+\delta^2+\varphi}, \tag{38}$$

where ratio of load or stress frequency to the frequency of natural vibrations is

$$\delta=\frac{\omega_\sigma}{\omega}=\omega_\sigma T_{\mathrm{K}}^{\mathrm{D}}. \tag{39}$$

Dynamic mechanical properties indicate the ability of a material to dissipate energy. Owing to their viscoelastic nature, dynamic mechanical properties measure the in-phase and out-of-phase modules with an applied oscillatory stress function. More importantly, $\tan\alpha$ the damping factor (measure of the phase angle between the applied stress and subsequent strain) is also obtained. This allows a qualitative estimation of the ability to dissipate energy.

The maximum phase angle is measure of the maximum energy dissipation

$$\max_{\delta=\sqrt{1+\varphi}}\tan\alpha=\frac{\varphi}{2\sqrt{1+\varphi}}. \tag{40}$$

The variation of phase angle with δ (D for the ratio δ) is shown in Fig. 3. At very high frequencies the behavior is stiff and elastic; the stress and strain are in phase. Lower frequencies allow some viscous flow, and the strain lags the stress. At still-lower frequencies, the stress and strain are again in phase.

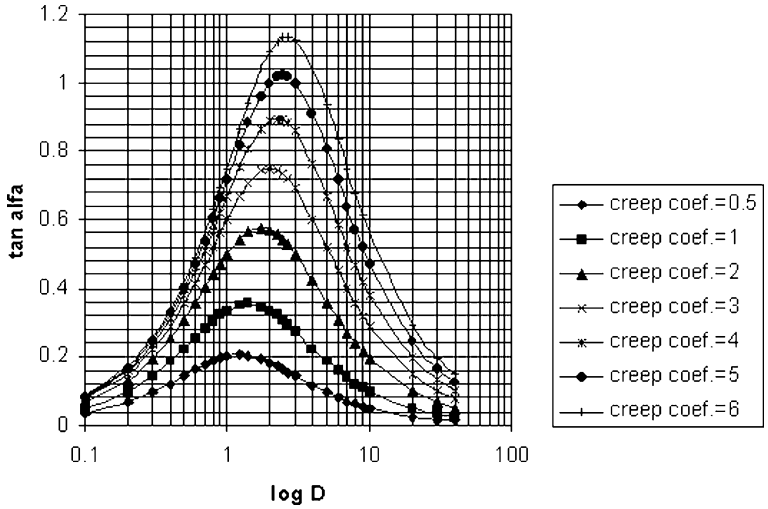

Fig. 3. Frequency dependence of phase angle.

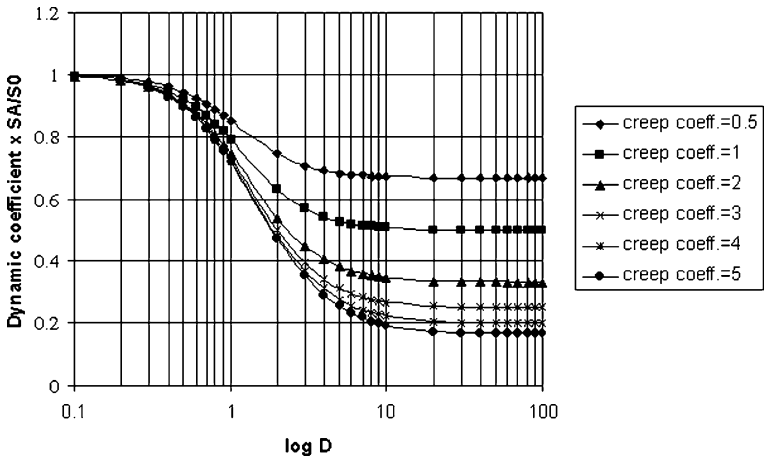

Fig. 4. RDA dynamic coefficient versus ratio δ.

The ratio η of cyclic strain amplitude ε_A to strain ε^c is the RDA dynamical coefficient,

$$\eta = \frac{\varepsilon_A}{\varepsilon^c} = \frac{\sigma_A}{\sigma_0}\sqrt{\frac{(1+\varphi)^2+\delta^2}{1+\delta^2}}\frac{1}{1+\varphi}. \tag{41}$$

This form of the formula shows that dynamic stresses may be expressed through constant stresses by multiplying the later with the RDA dynamic coefficient

$$\sigma_A = \eta\sigma_0. \tag{42}$$

At $\delta \to 0$ (static loading) or $\varphi \to 0$ (state of elasticity), we have the special case

$$\eta = \frac{\sigma_A}{\sigma_0}. \tag{43}$$

At $\delta \to \infty$ or $\delta \to 100$, the diagram representing the RDA dynamical coefficient becomes a horizontal line, as illustrated in Fig. 4, and

$$\lim_{\delta\to\infty}\eta = \frac{\sigma_A}{\sigma_0}\frac{1}{1+\varphi}. \tag{44}$$

5. Fatigue limit using RDA

5.1. Fatigue limit under constant stress amplitude

The ratio r is a key to understanding the loading mode for determination the fatigue limit in an asymmetrical cycle, which involves combination of tensile and compressive stresses, for example $r = -1$ represents reversed loading or symmetrical cycle. Other than quasi-static tensile and compressive stresses, where r is equal to one, the r ratio identifies the fatigue limit-loading mode in the range -1 and $+1$. In accordance with RDA the fatigue limit under constant stress amplitude may be obtained as follows:

$$\sigma_e = \sigma_0 + \sigma_A = \sigma_0 + \eta\sigma_0 = \sigma_0 + \sigma_A\sqrt{\frac{(1+\varphi)^2+\delta^2}{1+\delta^2}}\frac{1}{1+\varphi}. \tag{45}$$

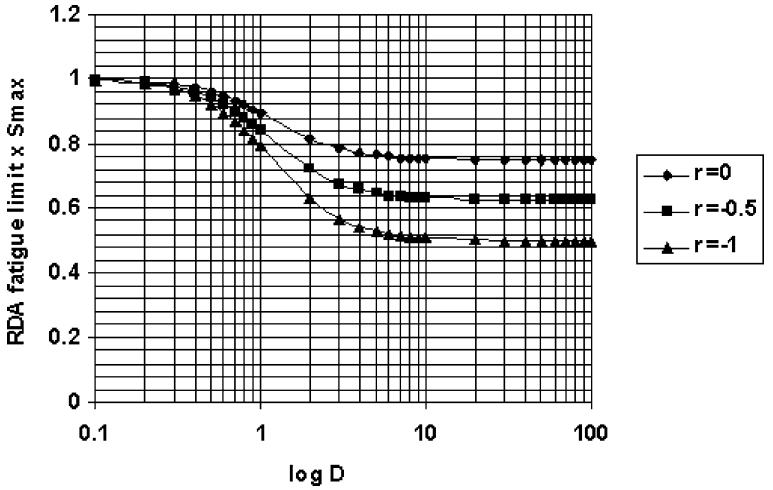

Fig. 5. RDA fatigue limit curves (S–$\log D$ curves) for creep coefficient = 1.

Taking into account formulas (24) and (25) we have

$$\sigma_e(r) = \frac{1}{2}\sigma_{max}\left[1 + r + (1-r)\sqrt{\frac{(1+\varphi)^2+\delta^2}{1+\delta^2}}\frac{1}{1+\varphi}\right]. \tag{46}$$

The results of formula (46) may be plotted on diagrams in which values of stress are plotted as ordinates and values of δ are plotted as abscissas. Such diagrams may be called S–D diagrams (S for stress, D for the ratio δ) and drawn using semi logarithmic plotting as shown in Fig. 5.

S–D diagrams become horizontal when $\delta \to \infty$ or $\delta \to 100$, for values of, φ ranging from 0.5 to 6, thus indicating a well-defined RDA fatigue limit as shown in Table 1. From formula (46) follows:

$$\lim_{\delta\to\infty}\sigma_e(1) = \sigma_{max}, \quad \lim_{\delta\to\infty}\sigma_e(0) = \frac{1}{2}\left(1+\frac{1}{1+\varphi}\right)\sigma_{max}, \quad \lim_{\delta\to\infty}\sigma_e(-1) = \frac{1}{1+\varphi}\sigma_{max}. \tag{47}$$

The proposed S–N curves are based on extensive theoretical studies using a newly proposed rheological model and RDA. Unlike previously available and purely empirical S–N curves, the newly developed S–N curves

Table 1
Numerical values depicting the variation of fatigue limit as a function of δ for various values of the creep coefficient φ

$\sqrt{\frac{(1+\varphi)^2+\delta^2}{1+\varphi}}\frac{1}{1+\varphi}$				
φ	δ			$1/(1+\varphi)$
	1	10	100	
0.5	0.849837	0.670779	0.666708	0.666667
1	0.790569	0.507371	0.500075	0.5
2	0.745356	0.346283	0.333467	0.333333
3	0.728869	0.267922	0.250187	0.25
4	0.72111	0.222497	0.20024	0.2
5	0.71686	0.1934	0.166958	0.166667
6	0.714286	0.173514	0.1432	0.142857

take into account the mechanical aspects of fatigue and cater for the influence of creep (creep coefficient) of material on the fatigue limit.

5.2. General variation of strength with range of stress

The test results for determining fatigue limit under different cycles are conveniently represented in the form of diagrams.

The simplest among these diagrams is the diagram in the σ_0 and σ_A coordinates (Haigh type of diagram) shown in Fig. 6. On this diagram the values of σ_0 are laid off on the x-axis to a certain scale and the values of σ_A are laid off on the y-axis in the same scale. Curves may be plotted on the basis of the formulas (47) as RDA fatigue limits under different cycles of variable stresses and for different values of creep coefficient.

Fig. 7 shows the Smith type of diagram in which the line representing constant (mean) stresses is drawn as a straight line at an angle of 45% with the horizontal axis. This makes the minimum stress line curve and permits the horizontal axis to represent the constant stresses to the same scale as on the vertical axis.

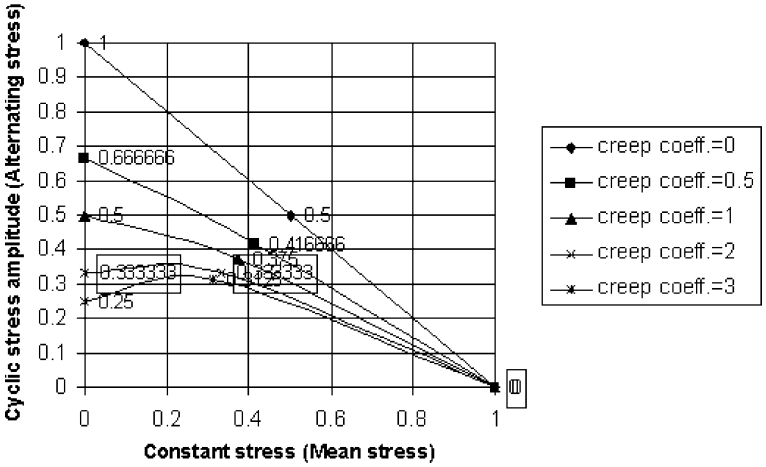

Fig. 6. Haigh type of diagram of RDA fatigue limits for different values of creep coefficients.

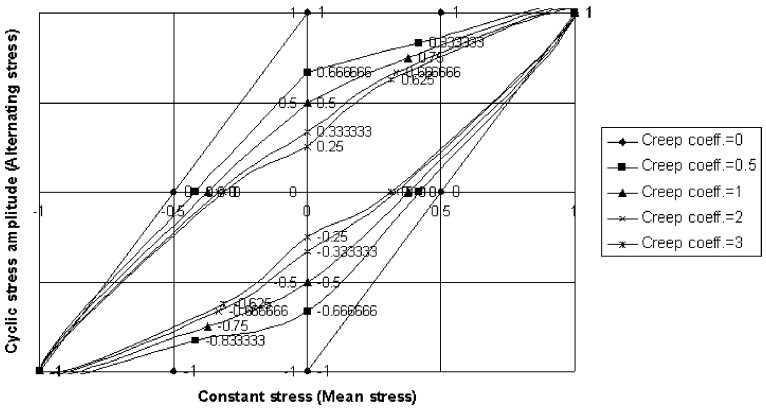

Fig. 7. Smith type of diagram of RDA fatigue limits for different values of creep coefficients.

6. Parameters of a new rheological model

Generally, the stress–strain curve is linear elastic until $\sigma \leqslant \sigma_{\mathrm{p}}$ (see Fig. 8) and nonlinear with considerable viscoelasto-plastic strain, under compression stress $\sigma \geqslant \sigma_{\mathrm{p}}$. Critical stresses and proportional stress are defined by Euler's expression

$$\sigma_{\mathrm{cr}} = \frac{E_{\mathrm{H}}\pi^2}{\left(\frac{l_0}{k_z}\right)^2} \Rightarrow \sigma_{\mathrm{p}} = \frac{E_{\mathrm{H}}\pi^2}{\left(\frac{l_0}{k_z}\right)^2_{\mathrm{p}}}. \tag{48}$$

If we now turn to the consideration the dynamical time of retardation $T_{\mathrm{K}}^{\mathrm{D}}$, we shall have the dynamic viscoelastic modulus $E_{\mathrm{K}}^{\mathrm{D}}$ (see formula (36))

$$E_{\mathrm{K}}^{\mathrm{D}} = \frac{E_{\mathrm{H}}}{\varphi^*}, \tag{49}$$

where φ^* is structural creep coefficient.

Using the RDA modeling technique the proportional stress now may be expressed as follows

$$\sigma_{\mathrm{p}}^{\mathrm{RDA}} = H'^{\mathrm{D}} E_{\mathrm{H}} \frac{1}{R}, \tag{50}$$

where H'^{D} is the dynamic viscoplastic modulus, and $R = \mathrm{const}$ is the RDA dimensional parameter. Comparing the two expressions for σ_{p}, we get

$$R = \frac{\left(\frac{l_0}{k_z}\right)^2_{\mathrm{p}}}{\pi^2} H'^{\mathrm{D}}. \tag{51}$$

On the other hand, $k = E_{\mathrm{H}}A/l_0$ and $k = E_{\mathrm{K}}^{\mathrm{D}}\, H'^{D}/\gamma$. Therefore

$$H'^{\mathrm{D}} = \varphi^* \frac{A\gamma}{l_0}. \tag{52}$$

Let us determine the structural creep coefficient φ^* on the thin long reinforced steel bar with circular cross-sectional area A and length $l_0 = l_{\mathrm{p}} = \lambda_{\mathrm{P}} k_z$, where k_z is the radius of gyration and $\lambda_{\mathrm{P}} \sim 100$. Choice of

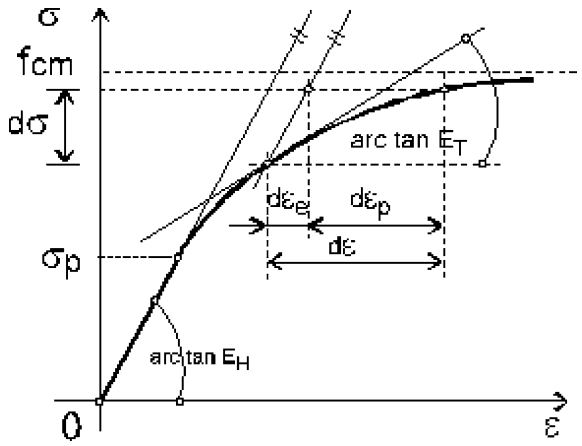

Fig. 8. Stress–strain curve.

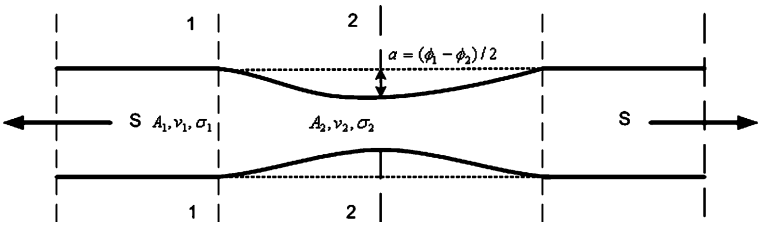

Fig. 9. Steady transfer of energy through a long bar having a section with reduced diameter.

slenderness ratio, $\lambda_P \sim 100$ can be explained by the fact that elastic (Euler's) theory is not valid for slenderness ratio under the 100. It is confirmed by numerous experimentally obtained results on steel.

During a small time interval Δt the total strain energy density will move so that the fictitious interface A_1 will have moved a short distance Δl_1. In the same time the fictitious interface A_2 will have moved a greater distance Δl_2 such that $A_1 \Delta l_1 = A_2 \Delta l_2 = V$, the fictitious volume. The energy went all the way through the fictitious volume without the physical transfer of material from the source by any cross-section of the bar in time Δt. Therefore (see Fig. 9),

$$A_1 v_1 = A_2 v_2, \tag{53}$$

where from

$$A_2 = A_1 \frac{v_1}{v_2}. \tag{54}$$

The reduced area A_2 can now be found by applying Bernoulli's energy theorem

$$\sigma_1 + \frac{1}{2}\rho v_1^2 = \sigma_2 + \frac{1}{2}\rho v_2^2 = \sigma_2 + \frac{1}{2}\rho \left(\frac{A_1}{A_2}\right)^2 v_1^2, \tag{55}$$

where $\sigma_1 = \sigma_p$ is the static energy density, and $1/2(\rho v_1^2)$ is the kinetic energy density.

By putting $v_1 = c$ (see formula (6)), in formula (55) we find that

$$A_2 = \frac{A_1}{\sqrt{\frac{2(\sigma_1 - \sigma_2)}{E_H} + 1}}. \tag{56}$$

Here σ_2 is the RDA fatigue limit in symmetrical cycle (see formula (47)),

$$\sigma_2 = \sigma_e(-1) = \frac{\sigma_p}{1 + \varphi^*}. \tag{57}$$

Thus we get the following formula for the reduced area A_2

$$A_2 = \frac{A_1}{\sqrt{\frac{2 \cdot \sigma_p}{E_H}\left(\frac{\varphi^*}{1+\varphi^*}\right) + 1}}. \tag{58}$$

If the bar is subjected to tensile or compressive stress in a given direction, not only strain in that direction (axial strain) takes place but also strains in directions perpendicular thereto (lateral strain). Within the range of elastic action the ratio of lateral to axial strain under conditions of uniaxial loading is called Poisson's ratio.

Experiments show that under tension (Fig. 9) the length of bar increases by Δl, whereas its width decreases by $2a = \Phi_1 - \Phi_2$. The axial strain can be found by applying Hooke's law

$$\varepsilon_{\mathrm{l}} = \frac{\sigma_{\mathrm{p}}}{E_{\mathrm{H}}}, \tag{59}$$

and the lateral strain is

$$\varepsilon_{\mathrm{t}} = \mu\varepsilon_{\mathrm{l}}, \tag{60}$$

where μ is Poisson's ratio.

On the other hand the lateral strain is

$$\varepsilon_{\mathrm{t}} = \frac{\phi_1 - \phi_2}{\phi_1}. \tag{61}$$

Therefore,

$$\mu = \frac{\phi_1 - \phi_2}{\phi_1}\frac{E_{\mathrm{H}}}{\sigma_{\mathrm{p}}}. \tag{62}$$

Diameter Φ_2 of the bar is

$$\phi_2 = \frac{\phi_1}{\sqrt[4]{\frac{2\sigma_{\mathrm{p}}}{E_{\mathrm{H}}}\left(\frac{\varphi^*}{1+\varphi^*}\right)+1}}. \tag{63}$$

Therefore, Poisson's ratio may be expressed by the formula

$$\mu = \left[1 - \frac{1}{\sqrt[4]{\frac{2\sigma_{\mathrm{p}}}{E_{\mathrm{H}}}\left(\frac{\varphi^*}{1+\varphi^*}\right)+1}}\right]\frac{E_{\mathrm{H}}}{\sigma_{\mathrm{p}}}. \tag{64}$$

For most structural materials, Poisson's ratio has values that lie between one-third and one-sixth; hence, with ordinary measuring devices, the precision of lateral-strain measurements is not as high as that of corresponding axial-strain measurements.

The influence of σ_{p} and E_{H} on the result of μ are very small as compared to φ^*. Then we may consider the theoretical value of Poisson's ratio ($\boldsymbol{\mu = 0.25}$) as the limit of formula (64), when $\varphi^* \to 1$,

$$\lim_{\varphi^*\to 1}\mu = \frac{E_{\mathrm{H}}\left(1 - \frac{1}{\sqrt[4]{\left(1+\frac{\sigma_{\mathrm{p}}}{E_{\mathrm{H}}}\right)}}\right)}{\sigma_{\mathrm{p}}} \approx 0.25. \tag{65}$$

Knowing the value of μ, we can calculate the change in the volume of the bar under tension or compression. If Poisson's ratio $\boldsymbol{\mu = 0.5}$, there is no change in the volume due to deformation. At $\varphi^* \to \infty$, then it will be

$$\lim_{\varphi^*\to \infty}\mu = \frac{E_{\mathrm{H}}\left(1 - \frac{1}{\sqrt[4]{\left(1+\frac{2\sigma_{\mathrm{p}}}{E_{\mathrm{H}}}\right)}}\right)}{\sigma_{\mathrm{p}}} \approx 0.5. \tag{66}$$

However, since $\mu < 0.5$ for a majority of the materials at small strains ($\varepsilon \ll 1$), tension is accompanied by an increase and compression by a decrease in the volume.

The value of extension ε was defined above as $\Delta l/l_0$, but it is not immaterial what the value of Δl is. If Δl is small, then it will be natural to refer it to l_0. But if Δl is not small, then at large extension ratios it will be

more logical to refer an infinitesimal change of the length $\mathrm{d}l$ to the current value of the length l. This means that an infinitesimal extension $\mathrm{d}\varepsilon^{\mathrm{H}}$ determined in this way is given by

$$\mathrm{d}\varepsilon^{\mathrm{H}} = \frac{\mathrm{d}l}{l}. \tag{67}$$

Then, proceeding from the natural initial condition of the absence of deformation at $l = l_0$, we obtain the following expression for ε^{H}

$$\varepsilon^{\mathrm{H}} = \int_{l_0}^{l} \frac{\mathrm{d}l}{l} = \ln\frac{l}{l_0} = \ln\frac{l_0 + \Delta l}{l_0} = \ln(1+\varepsilon). \tag{68}$$

The quantity ε^{H} as a measure of strain was first introduced by Roentgen; in the modern rheological literature it is called Hencky's measure of extension.

We now return to the concept of Poisson's ratio which we shall define as the ratio of lateral to axial strains. When an incompressible body is extended, in which case no change in volume occurs,

$$\mu^{\mathrm{H}} = 0.5. \tag{69}$$

We have discussed above some measures of small and large strains. This discussion shows that we may use E_{H} and μ as constants and obtain the following expression for the φ^* as a new constant or characteristic of the strained state

$$\varphi^* = \frac{\left[\left(\frac{1}{1-\frac{\mu\sigma_{\mathrm{p}}}{E_{\mathrm{H}}}}\right)^4 - 1\right]\frac{E_{\mathrm{H}}}{2\sigma_{\mathrm{p}}}}{1 - \left[\left(\frac{1}{1-\frac{\mu\sigma_{\mathrm{p}}}{E_{\mathrm{H}}}}\right)^4 - 1\right]\frac{E_{\mathrm{H}}}{2\sigma_{\mathrm{p}}}}. \tag{70}$$

The general approach to the analysis of the problem of the effect of Poisson's ratio on structural creep coefficient developing must also be based on formula (70). The form of the function $\varphi^*(\mu)$, assuming that the $\varepsilon_{\mathrm{p}} = \sigma_{\mathrm{p}}/E_{\mathrm{H}} = 0.001$ is shown in Fig. 10. Assuming μ equal to 1/3 for steel, we obtain $\varphi^* \sim 2$.

Results of a new rheological model parameters obtained here identify an important relationship $\boldsymbol{\varphi}^*(\boldsymbol{\mu})$ in the rheology, which have not been considered before.

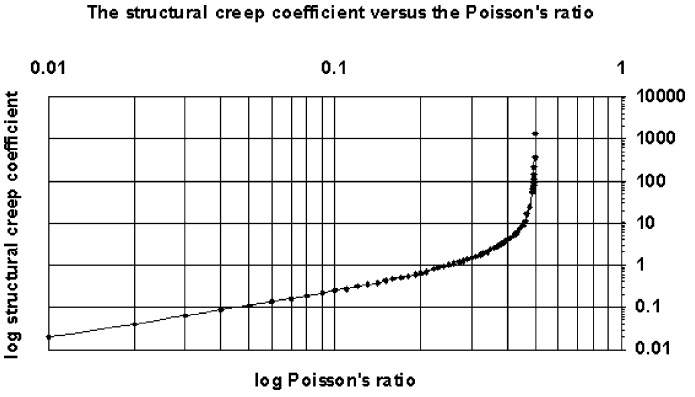

Fig. 10. Dependence of creep coefficient on the Poisson's ratio.

7. Hysteretic energy dissipation

7.1. The rate of release of viscoelastic energy

The phenomenon of hysteresis, which occurs in various branches of physics, (the lagging of the magnetization behind the magnetizing force is known as hysteresis) has been a long-standing topic of research interest (Lubarda et al., 1992). This paper focuses on the application of the new rheological model to the description of the hysteretic response of materials subjected to cyclic stress. When model is stretched, the elastic potential energy is stored in the material, as shown in Fig. 11.

The work required to stretch or compress a model does not depend on the weight of the model. Consequently, gravity is not involved in the measurement of elastic potential energy. Instead, the work required for the stretching or compressing is dependent upon the elasticity of the model, E_{H},

$$U_1 = \frac{\sigma_{\max}^2}{2E_{\mathrm{H}}} A l_0, \tag{71}$$

where $A = A_1$ (see Fig. 9).

Consider a elliptical loop of the rheological dynamical model shown in Fig. 11, where

$$\sigma''(t) = c\dot{\varepsilon}_{\mathrm{p}}''(t) = c\omega_\sigma \varepsilon_{\mathrm{A}} \cos(\omega_\sigma t - \alpha). \tag{72}$$

For a cyclic stress variation along the entire loop, the rate of release of viscoelastic energy is equal to the area enclosed by the loop, i.e.

$$W_{\mathrm{d,ve}} = \pi c \omega_\sigma \varepsilon_{\mathrm{A}}^2 \left[\frac{J}{M^2}\right]. \tag{73}$$

If $T_{\mathrm{K}}^{\mathrm{D}} = 1/\omega$ then the damping c (see formula (19)) is given by

$$c = 2kT_{\mathrm{K}}^{\mathrm{D}} = c_{\mathrm{c}}. \tag{74}$$

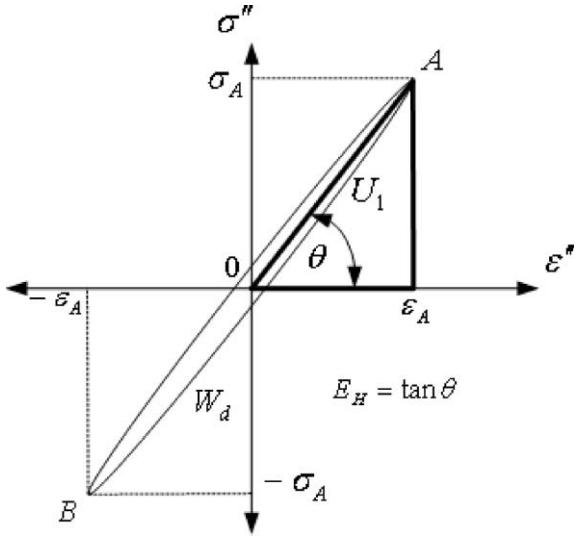

Fig. 11. Elastic potential energy and hysteretic loop dissipation in terms of stress–strain diagram.

Thus the rate of release of viscoelastic energy is given by

$$W_{\mathrm{d,ve}}(r) = \pi k \frac{1}{E_{\mathrm{H}}^2} \frac{(1-r)^2}{2} \sigma_{\max}^2 \frac{(1+\varphi^*)^2 + \delta^2}{1+\delta^2} \delta. \tag{75}$$

If the area of transfer of energy is cross sectional area A, then the energy dissipation is given by

$$U_{\mathrm{d}} = A W_{\mathrm{d,ve}}. \tag{76}$$

In the special case, at $\varphi^* \to 0$, we have elastic behavior and the rate of release of elastic energy from formula (75) as follows

$$W_{\mathrm{d,el}}(r) = \pi k \frac{1}{E_{\mathrm{H}}^2} \frac{(1-r)^2}{2} \sigma_{\max}^2 \delta. \tag{77}$$

As a result the first law of thermodynamics: when heat is converted to another form of energy, or when other forms of energy are converted to heat, there is no loss of energy, we have

$$U_2 - U_1 = Q - W, \tag{78}$$

where $U_2 - U_1$ is change in internal energy, Q is heat energy, and W is potential energy of the external loads.

A process in which no heat is added to or removed from a substance is called an adiabatic process. In such a case: $Q = 0$ and $U_2 = -W + U_1$. When the cyclic loading in an ideal elastic well-isolated system permits no heat to enter or leave during the process, the work done on the system equals the change in the internal energy.

7.2. Fatigue life prediction

It can easily be shown that the total potential energy of the system, $\Pi = U_2 = U_1 - W$ decreases as a temperature of the system rise. When all elastic potential energy is converted through hysteretic loop dissipation, we have

$$U_{\mathrm{d}} = U_1, \tag{79}$$

and relative frequency δ_{e} for theoretical estimation of the fatigue life is

$$\frac{(1+\varphi^*)^2 + \delta_{\mathrm{e}}^2(r)}{1+\delta_{\mathrm{e}}^2(r)} \delta_{\mathrm{e}}(r) = U_1 \frac{2E_{\mathrm{H}}^2}{A\pi k(1-r)^2 \sigma_{\max}^2} = \frac{l_0 E_{\mathrm{H}}}{\pi k (1-r)^2}. \tag{80}$$

Number of cycles for fatigue life is

$$N_{\mathrm{e}}(r) = \frac{\delta_{\mathrm{e}}(r)}{\delta_1}, \tag{81}$$

where $\delta_1 = 2\pi T_{\mathrm{K}}^{\mathrm{D}}/t_{\mathrm{p}}$ is the relative frequency for the first cycle, and t_{p} is time (s) when stress σ_{p} has been achieved.

7.3. Change in the temperature of the body

High cycle frequencies during the cycling process cause significant temperature rise in the isolated body and thermal expansion work, W_{T} as follows

$$W_{\mathrm{T}} = \frac{E_{\mathrm{H}}(\alpha_{\mathrm{T}} \Delta T)^2}{2} A l_0, \tag{82}$$

where α_{T} is a coefficient of linear thermal expansion, and ΔT [°C] is the difference between the final temperature and the original temperature of the specimen.

As mentioned above, elastic potential energy has to be converted into the thermal expansion work

$$U_{\mathrm{d}} = W_{\mathrm{T}}. \tag{83}$$

Difference between the final temperature and the original temperature is given by

$$\Delta T_{\mathrm{ve}} = \frac{1}{\alpha_{\mathrm{T}}}\sqrt{\frac{1}{\delta_{\mathrm{e}}(r)}\frac{(1+\varphi^*)^2+\delta^2}{1+\delta^2}\delta}\frac{\sigma_{\max}}{E_{\mathrm{H}}}. \tag{84}$$

In the special cases at $\varphi^* \to 0$ (state of elasticity), we have

$$\Delta T_{\mathrm{el}} = \frac{1}{\alpha_{\mathrm{T}}}\sqrt{\frac{\delta}{\delta_{\mathrm{e}}(r)}}\frac{\sigma_{\max}}{E_{\mathrm{H}}}, \tag{85}$$

where $\delta = \delta_1 N$ (N is the number of cycles).

7.4. Fatigue failure life prediction

We define the total mechanical energy as

$$U_{\mathrm{T}} = -W + U_{\mathrm{e}} + U_{\mathrm{s}} = \Pi + U_{\mathrm{s}}, \tag{86}$$

where $U_{\mathrm{s}} = 2\gamma_{\mathrm{s}}A_{\mathrm{s}}$ is the necessary energy to produce a unit area of fracture surface, γ_{s} is the specific surface energy, and A_{s} is the fracture or crack area.

For the Griffith equilibrium state, the rate of release of potential energy is given by

$$G_{\mathrm{I}} = G_{\mathrm{cr}} = 2\gamma_{\mathrm{s}}. \tag{87}$$

The relative frequency for the fatigue failure life can be most simply explained by the RDA model, which assumes that the all energy for any fixed crack area is converted through hysteretic loop dissipation

$$U_{\mathrm{d}} = U_{\mathrm{T}} = -W + U_{\mathrm{e}} + U_{\mathrm{s}} = \Pi + U_{\mathrm{s}} \Rightarrow \frac{(1+\varphi^*)^2+\delta_{\mathrm{c}}^2(r)}{1+\delta_{\mathrm{c}}^2(r)}\delta_{\mathrm{c}}(r) = (\Pi + U_{\mathrm{s}})\frac{2E_{\mathrm{H}}^2}{A_{\mathrm{s}}\pi k(1-r)^2\sigma_{\max}^2}. \tag{88}$$

Let us now write down the expression for δ_{c} in the case of axial loading and $A_{\mathrm{s}} = A$

$$\frac{(1+\varphi^*)^2+\delta_{\mathrm{c}}^2(r)}{1+\delta_{\mathrm{c}}^2(r)}\delta_{\mathrm{c}}(r) = \left(-1+\frac{G_{\mathrm{I}}}{\frac{\sigma_{\max}^2}{2E_{\mathrm{H}}}l_0}\right)\delta_{\mathrm{e}}(r). \tag{89}$$

8. Fatigue failure

8.1. The localized reduction of cross-sectional area

Let us calculate the localized reduction of cross-sectional area in center of specimen, (Fig. 9) taking into account the creep of steel. Initial strain rate takes into consideration delayed elastic is $\sigma_1/\lambda_{\mathrm{K}}$ or

$$\dot{\varepsilon}_1 = v\frac{\varphi^*}{l_0} = \frac{\sigma_1}{\sqrt{E_{\mathrm{H}}\rho}}\frac{\varphi^*}{l_0}, \tag{90}$$

where $v_1 = v$ is the velocity of the particles (see formula (7)).

In this case we can directly apply Bernoulli's energy theorem

$$\sigma_1 + \frac{1}{2}\rho A^* l_0\dot{\varepsilon}_1^2\frac{1}{l_0} = \sigma_2 + \frac{1}{2}\rho A^* l_0\dot{\varepsilon}_2^2\frac{1}{l_0} = \sigma_2 + \frac{1}{2}\rho A^*\left(\frac{A_1}{A_{\mathrm{red}}}\right)^2\dot{\varepsilon}_1^2, \tag{91}$$

where $A^* = 1$ is a unit cross-sectional area, $\sigma_1 = \sigma_{\max}$ and σ_2 is the RDA fatigue limit in symmetrical cycle (see formula (57)).

Therefore, the localized reduction of cross-sectional area in center of specimen and reduced diameter are:

$$A_{\text{red}} = \frac{A_1}{\sqrt{\dfrac{2E_{\text{H}}l_0^2}{\sigma_{\max}A^*\varphi^*}\dfrac{1}{1+\varphi^*}+1}}, \quad \frac{\phi_1}{\phi_{\text{red}}} = \sqrt[4]{\frac{2E_{\text{H}}l_0^2}{\sigma_{\max}A^*\varphi^*}\frac{1}{1+\varphi^*}+1}. \tag{92}$$

8.2. The RDA fracture stress

Let the fracture stress be denoted by σ_{c} and the cross-sectional area in the narrowest section by A_{red}, then

$$\sigma_{\text{c}} = \frac{S_2}{A_{\text{red}}} = \sigma_2\frac{A_1}{A_{\text{red}}}, \tag{93}$$

where $S_2 = S_1/(1+\varphi^*)$ and $S_1 = \sigma_1 A_1$. Further yields

$$\sigma_{\text{c}} = \frac{\sigma_{\max}}{(1+\varphi^*)}\sqrt{\frac{2E_{\text{H}}l_0^2}{\sigma_{\max}A^*\varphi^*}\frac{1}{1+\varphi^*}+1}, \tag{94}$$

where $\sigma_{\max}$ is maximum absolute stress in the cycle.

8.3. The maximum applied dynamical stress

Considering the relationship between σ_{c} and $\sigma_{\max}$ earlier obtained from condition of fracture, we can now obtain the maximum applied dynamical stress in symmetrical cycle ($r = -1$), which results from the fact that we provide the total fatigue failure life of the bar under axial loading.

$$\sigma_{\max,\text{c}} = \frac{E_{\text{H}}l_0^2}{A^*\varphi^*(1+\varphi^*)}\left[-1+\sqrt{1+\frac{\sigma_{\text{c}}^2A^{*2}\varphi^{*2}(1+\varphi^*)^4}{E_{\text{H}}^2l_0^4}}\right]. \tag{95}$$

In the above formula, σ_{c} is the ultimate or fracture strength under quasi-static loading.

8.4. The RDA rate of release of potential energy

Fracture by the progressive growth of incipient flaws under cyclically varying loads may be formulated by follow condition

$$\frac{\delta_{\text{c}}(-1)}{\delta_{\text{e}}(-1)} = \frac{\phi_1}{\phi_{\text{red}}} = \sqrt[4]{\frac{2E_{\text{H}}l_0^2}{\sigma_{\max,\text{c}}A^*\varphi^*}\frac{1}{1+\varphi^*}+1}. \tag{96}$$

It is based on the assumption that in period from the fatigue life to the fatigue failure life the reduction of the cross-section area goes on.

Then, according to above assumption, the RDA rate of release of potential energy will be (see (89))

$$G_{\text{I,c}} = \left(\frac{\phi_1}{\phi_{\text{red}}}+1\right)\frac{\sigma_{\max,\text{c}}^2l_0}{2E_{\text{H}}}, \quad G_{\text{I,c}} = \left(\sqrt[4]{\frac{2E_{\text{H}}l_0^2}{\sigma_{\max,\text{c}}A^*\varphi^*}\frac{1}{1+\varphi^*}+1}+1\right)\frac{\sigma_{\max,\text{c}}^2l_0}{2E_{\text{H}}}, \tag{97}$$

where from the RDA stress intensity factor yields

$$K_{\text{I,c}} = \sqrt{G_{\text{I,c}}E_{\text{H}}}. \tag{98}$$

9. Comparison of experimental and computational results

9.1. Experimental data

Axial fatigue experiment was performed. Temperature data on reinforcing steel bar, $\Phi = 19$ mm are used for their comparison with the RDA results. For a more exact elucidation of the RDA, difference between the final temperature and the original temperature on reinforcing steel bar was investigated, ΔT [°C]. The specimen is loaded at the original temperature of 19 °C, with cyclic sinusoidal load in a symmetrical cycle: $\sigma_0 = 0$, $\sigma_{\max} = 141$ MPa, and frequency, $f = f_\sigma = 20$ Hz. The specimen on which, the work was done was an isolated reinforced steel bar to reduce the transfer of heat to a minimum. Temperatures of the specimen under unchanged conditions at ambient temperature are measured after: 10^4 (8.33 min), 10^5 (1.388 h), 2×10^5 (2.77 h), 3×10^5 (4.166 h), 4×10^5 (5.55 h) and 5×10^5 (6.944 h) cycles and shown in Table 2 and Fig. 12.

Table 2
The variations RDA results with number of cycles and test data of temperatures on isolated reinforced steel bar

Number of cycles N	Relative frequency δ	$\sigma_e(-1)$ (MPa)	ΔT_{el} (°C)	ΔT_{ve} (°C)	α (rad)	$W_{d,ve}$ (J/m^2)	$W_{d,el}$ (J/m^2)	ΔT (°C) test data
1	0.000000889	141	0.0060462	0.0181385	5.9267E–07	0.002698789	0.000299865	
10	0.00000889	141	0.0191197	0.057359	5.9267E–06	0.02698789	0.002998654	
100	0.0000889	141	0.0604617	0.1813851	5.9267E–05	0.269878897	0.029986544	
1000	0.000889	140.99995	0.1911967	0.5735889	0.00059267	2.69878709	0.299865443	
10 000	0.00889	140.99505	0.6046171	**1.8137876**	0.00592644	26.985998409	2.998654429	**1.5**
100 000	0.0889	140.50776	1.9119671	**5.7158768**	0.05904224	267.9978453	29.98654429	**5.2**
200 000	0.1778	139.06638	2.7039298	**8.0005474**	0.11676375	525.0552298	59.97308857	**6.7**
300 000	0.2667	136.7753	3.3116242	**9.6371995**	0.71796661	761.8461533	89.95963286	**7.2**
400 000	0.3556	136.78044	3.8239343	**10.884417**	0.22367212	971.7977983	119.9461771	**8**
500 000	0.4445	130.25138	4.2752885	**11.848133**	0.27117424	1151.503824	149.9327214	**8.2**
600 000	0.5334	126.35947	4.6833439	12.591167	0.31404806	1300.461648	179.9192657	
700 000	0.6223	122.26122	5.0585895	13.158921	0.35212271	1420.385288	209.90581	
800 000	0.7112	118.08858	5.4078597	13.587371	0.38543369	1514.385581	239.8923543	
900 000	0.8001	113.94542	5.7359014	13.905951	0.4141684	1586.232898	269.8788986	
1 000 000	0.889	109.9084	6.0461709	14.138829	0.43861491	1639.805902	299.8654429	
1948313.62	**1.732050807**	**81.406388**	**8.4393666**	**14.617412**	**0.52359878**	**1752.695779**	**584.2319262**	
2 000 000	1.778	80.347782	8.5505769	14.617445	0.52345038	1752.703643	599.7308857	
3 000 000	2.667	66.236412	10.472275	14.758424	0.48536234	1786.674979	899.5963286	
4 000 000	3.556	59.195553	12.092342	15.230061	0.42665793	1902.693617	1199.461771	
5 000 000	4.445	55.32028	13.519649	15.912995	0.37240403	2077.157606	1499.327214	
6 000 000	5.334	53.000342	14.810034	16.700784	0.32701074	2287.91187	1799.192657	
7 000 000	6.223	51.515534	15.996665	17.533547	0.28987916	2521.768148	2099.0581	
8 000 000	7.112	50.513462	17.101154	18.379542	0.25948437	2770.989963	2398.923543	
9 000 000	8.001	49.80773	18.138513	19.222088	0.23438997	3030.865883	2698.788986	
10 000 000	8.89	49.293117	19.119671	20.052515	0.21344291	3298.399599	2998.654429	
20 000 000	17.78	47.589128	27.039298	27.378226	0.11097073	6148.599221	5997.308857	
30 000 000	26.67	47.263201	33.116242	33.301694	0.07453732	9097.000528	8995.963286	
40 000 000	35.56	47.148322	38.239343	38.360018	0.05605108	12070.44222	11994.61771	
50 000 000	44.45	47.095007	42.752885	42.839306	0.04489597	15053.94901	14993.27214	
60 000 000	53.34	47.066008	46.833439	46.899212	0.03743832	180402.49844	17991.92657	
70 000 000	62.23	47.048509	50.585895	50.638105	0.03210293	21033.93236	20990.581	
78 928 009	**70.167**	**47.038162**	**53.715051**	**53.758665**	**0.02847837**	**23706.23212**	**23667.78237**	
80 000 000	71.12	47.037146	54.078597	54.121338	0.02809742	24027.17016	23989.23543	
90 000 000	80.01	47.029354	57.359014	57.394837	0.02497997	27021.61102	26987.88986	
100 000 000	88.9	47.023779	60.461709	60.492299	0.02248486	30016.89423	29986.54429	

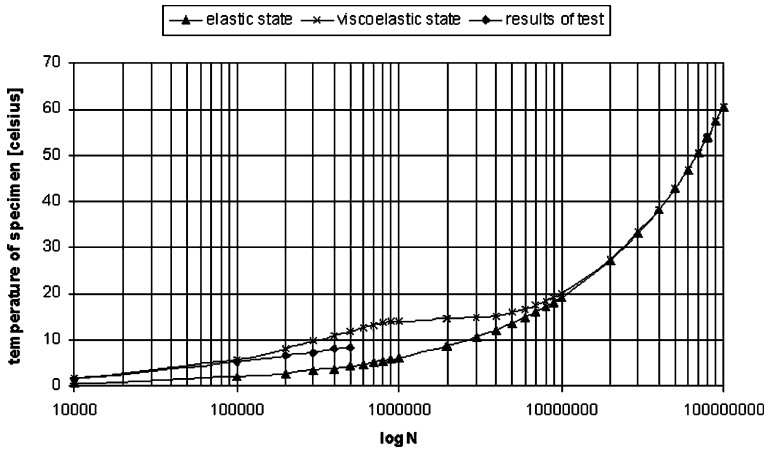

Fig. 12. Computational RDA results of temperatures on testing bar and test data $<5 \times 10^5$ cycles.

9.2. RDA fatigue results

Material isotropic: elastic modulus, $E_H = 2.1 \times 10^5$ MPa; Poisson's ratio, $\mu = 1/3$; specific gravity, $\gamma = 7.86 \times 10^{-3}$ kg/cm^3; coefficient of linear thermal expansion, $\alpha_T = 125 \times 10^{-7}$ °C^{-1}.

Isolated reinforced steel bar ($l_0 = 50$ cm, $\Phi = 1.9$ cm):

$$I_z = \frac{\phi^4\pi}{64}, \quad A = \frac{\phi^2\pi}{4}, \quad k_z = \sqrt{\frac{I_z}{A}} = \frac{\phi}{4}, \quad \frac{l_0}{k_z} = \frac{l_0}{\frac{\phi}{4}} = \frac{4 \times 50}{1.9} = 105.26.$$

Proportional stress:

$$\sigma_p^E = \frac{E_H\pi^2}{\left(\frac{l_0}{k_z}\right)_p^2} = \frac{2.1 \times 10^5 \times \pi^2}{105.26^2} = 187.06 \text{ MPa} > 141 \text{ MPa}.$$

Structural creep coefficient:

$$\varphi^* = \frac{\left[\left(\frac{1}{1-\frac{\mu\sigma_p}{E_H}}\right)^4 - 1\right]\frac{E_H}{2\sigma_p}}{1 - \left[\left(\frac{1}{1-\frac{\mu\sigma_p}{E_H}}\right)^4 - 1\right]\frac{E_H}{2\sigma_p}}, \quad \varphi^* = \frac{\left[\left(\frac{1}{1-\frac{0.333\times187.06}{210\,000}}\right)^4 - 1\right]\frac{210\,000}{2\times187.06}}{1 - \left[\left(\frac{1}{1-\frac{0.333\times187.06}{210\,000}}\right)^4 - 1\right]\frac{210\,000}{2\times187.06}} = 2.$$

RDA viscoelastic modulus:

$$E_K^D = \frac{E_H}{\varphi^*}, \quad E_K^D = \frac{2.1 \times 10^5}{2} = 1.05 \times 10^5 \text{ MPa}.$$

RDA viscoplastic modulus:

$$H'^D = \varphi^* \frac{A\gamma}{l_0}, \quad H'^D = 2\frac{1.9^2 \times \pi \times 7.86 \times 10^{-3}}{4 \times 50} = 0.000891 \text{ kg/cm}^2.$$

RDA dimensional parameter:

$$R = \frac{\left(\frac{l_0}{k_z}\right)_p^2}{\pi^2} H'^D, \quad R = \frac{105.26^2}{\pi^2} 0.000891 = 1 \text{ kg/cm}^2.$$

Dynamic time of retardation:

$$T_{\mathrm{K}}^{\mathrm{D}} = \sqrt{\frac{\rho}{E_{\mathrm{H}}}} l_0 = 0.5\sqrt{\frac{7860}{2.1\times 10^5 \times 10^6}} = 0.0000967 \text{ s}.$$

Original loading time:

Let us choose, $t = t_{\mathrm{p}}$ (t_{p} is time when proportional stress σ_{p} has been achieved) from creep data (Kojić, 1997):

$$\varepsilon^{\mathrm{c}} = a_0 \sigma_{\mathrm{p}}^{a_1} t_{\mathrm{p}}^{a_2}, \quad a_0 = 2.0\times 10^{-9}, \quad a_1 = 3.0, \quad a_2 = 1.2, \quad t_{\mathrm{p}}\ [\mathrm{h}], \quad E_{\mathrm{H}}[\mathrm{MPa}],$$

$$t_{\mathrm{p}} = 60\left(\sqrt[1.2]{\frac{\varphi^*}{2\times 10^{-9}\times \sigma_{\mathrm{p}}^2 \times E_{\mathrm{H}}}}\right) = 60\left(\sqrt[1..2]{\frac{2}{2\times 10^{-9}\times 187^2 \times 2.1\times 10^5}}\right) = 11.38 \text{ min} = 683 \text{ s}.$$

Relative frequency or ratio δ:

$$\delta = \frac{\omega_\sigma}{\omega} = 2\pi f T_{\mathrm{K}}^{\mathrm{D}} = 0.000607584\, f = 0.000607584 \frac{N}{t_{\mathrm{p}}} = 0.000000889 N.$$

Fatigue limit in a symmetrical cycle:

$$\sigma_{\mathrm{e}}(-1) = \sqrt{\frac{(1+\varphi)^2+\delta^2}{1+\delta^2}} \frac{1}{1+\varphi}\sigma_{\mathrm{A}} = \sqrt{\frac{9+\delta^2}{1+\delta^2}} \frac{1}{3} 141,$$

$$\lim_{\delta\to\infty} \sigma_{\mathrm{e}}(-1) = \frac{1}{1+\varphi}\sigma_{\mathrm{A}} = \frac{1}{3} 141 = 47 \text{ MPa}.$$

Relative frequency for theoretical estimation of the fatigue life, $r = -1$:

$$\delta_{\mathrm{e}}(-1) = \frac{l_0 E_{\mathrm{H}}}{\pi k (1-r)^2} = \left(\frac{l_0}{\phi\pi}\right)^2 = \left(\frac{50}{1.9\times\pi}\right)^2 = 70.167.$$

Number of cycles for the fatigue life:

$$N_{\mathrm{e}}(-1) = \frac{\delta_{\mathrm{e}}(-1)}{\delta_1} = \frac{70.167}{0.000000889} = 78\,928\,009 c.$$

Fatigue life:

$$t_{\mathrm{e}}(-1) = \frac{N_{\mathrm{e}}(-1)}{f_\sigma} = \frac{78\,928\,009}{20} = 3946400.45 \text{ s} = 45.6759 \text{ days}.$$

Change of temperature of the bar:

$$\Delta T_{\mathrm{el}} = \frac{1}{\alpha_{\mathrm{T}}}\sqrt{\frac{\delta}{\delta_{\mathrm{e}}(r)}}\frac{\sigma_{\max}}{E_{\mathrm{H}}} = \frac{1}{125\times 10^{-7}}\sqrt{\frac{\delta}{70.167}}\frac{141}{2.1\times 10^5},$$

$$\Delta T_{\mathrm{ve}} = \frac{1}{\alpha_{\mathrm{T}}}\sqrt{\frac{1}{\delta_{\mathrm{e}}(r)}\frac{(1+\varphi)^2+\delta^2}{1+\delta^2}\delta}\frac{\sigma_{\max}}{E_{\mathrm{H}}} = \frac{1}{125\times 10^{-7}}\sqrt{\frac{\delta}{70.167}\frac{9+\delta^2}{1+\delta^2}}\frac{141}{2.1\times 10^5}.$$

Phase angle:

$$\tan\alpha = \frac{\delta\varphi}{1+\delta^2+\varphi} = \frac{2\delta}{3+\delta^2}, \quad \max_{\delta=\sqrt{1+\varphi}} \tan\alpha = \frac{\varphi}{2\sqrt{1+\varphi}}, \quad \max_{\delta=1.732} \tan\alpha = \frac{2}{2\sqrt{3}} = 0.57735.$$

The rate of release of viscoelastic energy:

$$W_{\mathrm{d,ve}}(-1) = 2\pi k \frac{1}{E_{\mathrm{H}}^2}\sigma_{\max}^2 \frac{(1+\varphi)^2+\delta^2}{1+\delta^2}\delta = 2\pi \frac{0.000283528}{2.1\times 10^5 \times 0.5} 141^2 \frac{9+\delta^2}{1+\delta^2}\delta \times 10^6.$$

The rate of release of elastic energy:

$$W_{\mathrm{d,el}}(-1) = 2\pi k \frac{1}{E_{\mathrm{H}}^2}\sigma_{\max}^2 \delta = 2\pi \frac{0.000283528}{2.1\times 10^5 \times 0.5} 141^2 \delta 10^6.$$

Strength in tension: yield strength, $\sigma_{\mathrm{Y}} = 400$ MPa; ultimate strength, $\sigma_{\mathrm{c}} = 500$ MPa.

Maximum applied dynamical stress:

$$\sigma_{\max,\mathrm{c}} = \frac{E_{\mathrm{H}} l_0^2}{A^* \varphi^* (1+\varphi^*)} \left[-1 + \sqrt{1 + \frac{\sigma_{\mathrm{c}}^2 A^{*2} \varphi^{*2} (1+\varphi^*)^4}{E_{\mathrm{H}}^2 l_0^4}} \right],$$

$$\sigma_{\max,\mathrm{c}} = \frac{2.1\times 10^5 \times 0.5^2}{1\times 2\times (1+2)} \left[-1 + \sqrt{1 + \frac{500^2 \times 1 \times 2^2 \times (1+2)^4}{(2.1\times 10^5)^2 \times 0.5^4}} \right] = 127.64 \text{ MPa}.$$

Reduced diameter:

$$\frac{\phi_1}{\phi_{\mathrm{red}}} = \sqrt[4]{\frac{2E_{\mathrm{H}} l_0^2}{\sigma_{\max,\mathrm{c}} A^* \varphi^*} \frac{1}{1+\varphi^*} + 1}, \quad \frac{\phi_1}{\phi_{\mathrm{red}}} = \sqrt[4]{\frac{2\times 2.1\times 10^5 \times 0.5^2}{127.64 \times 1 \times 2} \frac{1}{1+2} + 1} = 3.427.$$

RDA rate of release of potential energy:

$$G_{\mathrm{I,c}} = \left(\frac{\phi_1}{\phi_{\mathrm{red}}} + 1 \right) \frac{\sigma_{\max,\mathrm{c}}^2 l_0}{2E_{\mathrm{H}}}, \quad G_{\mathrm{I,c}} = (3.427+1)\frac{127.64^2 \times 0.5}{2\times 2.1\times 10^5} = 0.08588 \text{ MJ/m}^2 = 85.88 \text{ kJ/m}^2.$$

RDA stress intensity factor:

$$K_{\mathrm{I,c}} = \sqrt{G_{\mathrm{I,c}} E_{\mathrm{H}}}, \quad K_{\mathrm{I,c}} = \sqrt{0.08588 \times 2.1 \times 100\,000} = 134.294 \text{ MN m}^{-3/2}.$$

Relative frequency for theoretical estimation of the fatigue failure life:

$$\delta_{\mathrm{c}}(-1) = \left(-1 + \frac{G_{\mathrm{I,c}}}{\frac{\sigma_{\max,\mathrm{c}}^2}{2E_{\mathrm{H}}} l_0} \right) \delta_{\mathrm{e}}(-1), \quad \frac{\sigma_{\max,\mathrm{c}}^2}{2E_{\mathrm{H}}} l_0 = \frac{127.64^2}{2\times 2.1\times 10^5} \times 0.5 = 0.019395201 \text{ MP/m}$$
$$= 19.40 \text{ kJ/m}^2,$$

$$\delta_{\mathrm{c}}(-1) = \left(-1 + \frac{85.88}{19.40} \right) 70.167 = 3.427 \times 70.167 = 240.45.$$

Number of cycles for the fatigue failure life:

$$N_{\mathrm{c}}(-1) = \frac{\delta_{\mathrm{c}}(-1)}{\delta_1} = \frac{240.45}{0.000000889} = 270\,470\,827c.$$

Fatigue failure life:

$$t_{\mathrm{c}}(-1) = \frac{N_{\mathrm{c}}(-1)}{f_\sigma} = \frac{270\,470\,827}{20} = 13\,523\,541 \text{ s} = 156.52 \text{ days}.$$

9.3. Griffith's theory of fracture results

For the classic Griffith's crack, the stress intensity factor is given by

$$K_{\mathrm{I}} = \sigma_{\mathrm{c}}\sqrt{\pi a}. \tag{99}$$

For other geometries the stress intensity factor can be written as

$$K_{\mathrm{I}} = \sigma_{\mathrm{N}}\sqrt{\pi a}F(a/b), \tag{100}$$

where σ_{N} is the nominal stress at the crack, and F is a geometric factor that depends upon the geometry of the specimen and can be found in stress intensity handbooks such as Tada et al. (1973) and Rooke and Cartwright (1976).

Consider a crack of the specimen shown in Fig. 16, where

$$\begin{aligned}
&F(a/b) = \sqrt{\frac{2b}{\pi a}\tan\left(\frac{\pi a}{2b}\right)},\\
&b = 19\ \text{mm}, \quad \phi_{\mathrm{red}} = \frac{\phi_1}{3.428} = \frac{19}{3.428} = 5.542\ \text{mm}, \quad a = \frac{19 - 5.542}{2} = 6.7287\ \text{mm},\\
&F(a/b) = \sqrt{\frac{2\times 19}{\pi\times 6.7287}\tan\left(\frac{\pi\times 6.7287}{2\times 19}\right)} = 1.05724,\\
&K_{\mathrm{I}} = 500\sqrt{\pi\frac{6.7287}{1000}}1.05724 = 76.8568\ \text{MN}\,\text{m}^{-3/2},\\
&G_{\mathrm{I}} = \frac{K_{\mathrm{I}}^2}{E_{\mathrm{H}}} = \frac{76.8568^2}{2.1\times 10^5} = 0.028128\ \text{MJ/m}^2 = 28.128\ \text{kJ/m}^2.
\end{aligned} \tag{101}$$

Because of the circular crack yields:

$$G_{\mathrm{I}}^* = 28.128\times\pi = 88.368\ \text{kJ/m}^2,$$

$$K_{\mathrm{I}}^* = \sqrt{G_{\mathrm{I}}^* E_{\mathrm{H}}} = \sqrt{0.088368\times 2.1\times 100\,000} = 136.225\ \text{MN}\,\text{m}^{-3/2}.$$

9.4. Discussion

Experimental data are shown for six different numbers of cycles. *There is a very good compatibility between the experimental data and the RDA results in the first three time periods (2.77 h), as shown in Fig.* 12. The RDA results are not well compatible with test data for the latter time periods (6.944 h). The reason for that is a contact between heads of the testing machine and specimen, which could not be isolated to prevent the flow of heat through a metal.

The phase angle between the applied stress and subsequent strain is shown in Fig. 13. The maximum phase angle, $\delta = 1.732$, $N \sim 2\times 10^6$ is measure of the maximum difference between the rate of release of viscoelastic energy and the rate of release of elastic energy (see Fig. 14). At very high frequencies, $\delta \sim 20$, $N\delta \sim 2\times 10^7$ the stress and strain are in phase. Frequencies between $\delta \sim 0.1$, $N \sim 2\times 10^5$ and ~ 20, $N \sim 2\times 10^7$ allow some viscous flow, the strain lags the stress, and this is range when the fatigue appears (see Fig. 15).

Relative frequency for the fatigue life is $\delta_{\mathrm{e}}(-1) = 70.167$, ($N_{\mathrm{e}}(-1) = 78928009c$ and $t_{\mathrm{e}}(-1) = 45.676$ days). This is a number of cycles when the elastic potential energy is converted through hysteretic loop dissipation. Relative frequency for the fatigue failure life is $\delta_{\mathrm{c}}(-1) = 240.45$, ($N_{\mathrm{c}}(-1) = 270470827c$ and

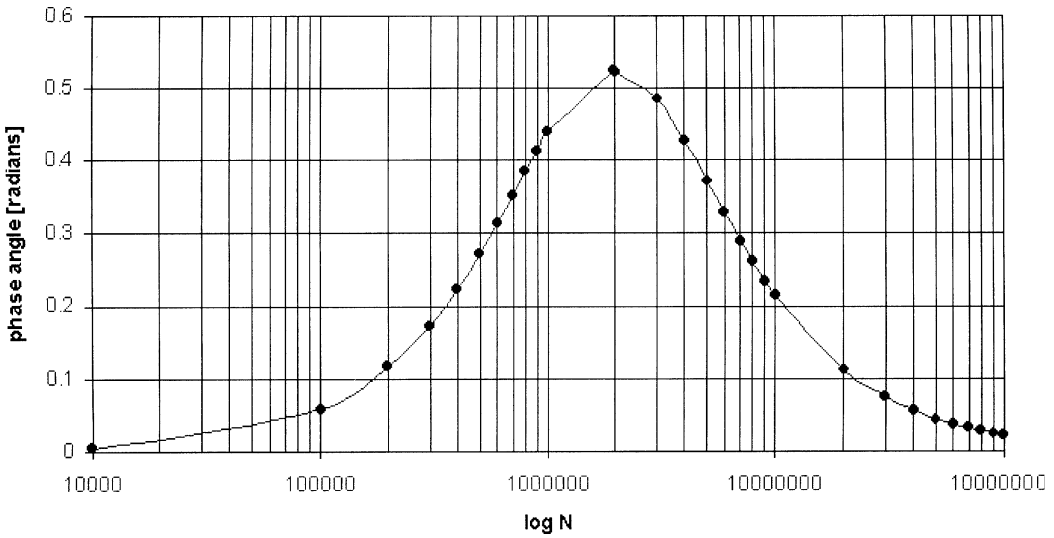

Fig. 13. Log$N$ dependence of phase angle of testing bar.

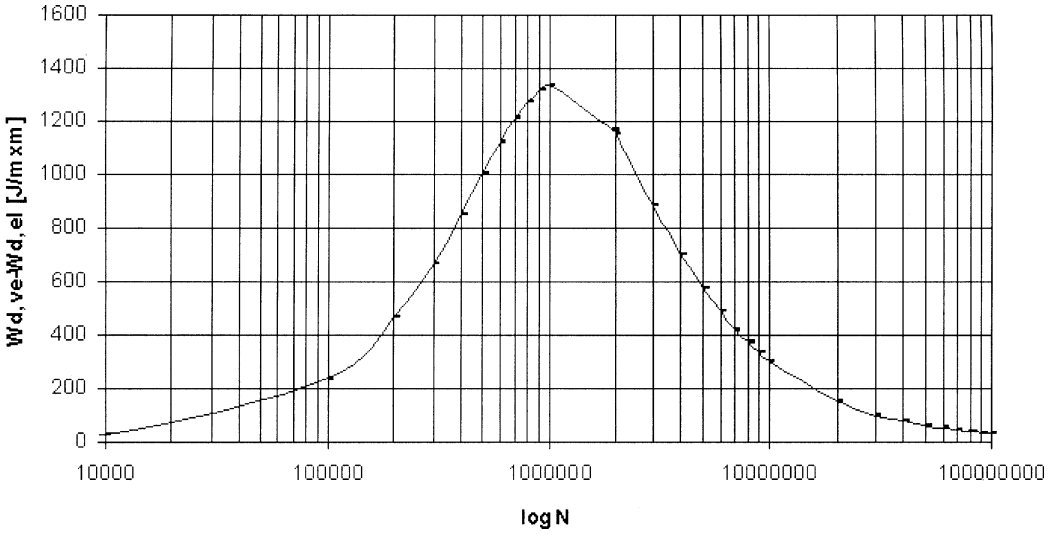

Fig. 14. Log$N$ dependence of difference between the rate of release of viscoelastic energy and the rate of release of elastic energy of testing bar.

$t_c(-1) = 156.52$ days). Although the RDA rate of release of potential energy, $G_{I,c} = 85.88$ kJ/m^2 is 4.427 times great as the rate of release of elastic energy, $W_{d,el}(-1) = 19.40$ kJ/m^2 the fatigue failure life is only 3.427 times long as fatigue life because some part of the total mechanical energy (elastic potential energy) is converted through hysteretic loop dissipation and remainder is stored in the material and produced failure.

Two various methods of determining the rate of release of potential energy, G_I have been analyzed. The emphasis has been to show that RDA method enables the rate of release of potential energy to be calculated from this theory, differently obtained by Griffith theory, or experimentally. On the basis of the comparison, the present method is regarded as valid and suitable (RDA: $G_{I,c} = 85.88$ kJ/m^2, $K_{I,c} = 134.294$ MN m$^{-3/2}$; Griffith: $G_I = 88.368$ kJ/m^2, $K_I = 136.225$ MN m$^{-3/2}$).

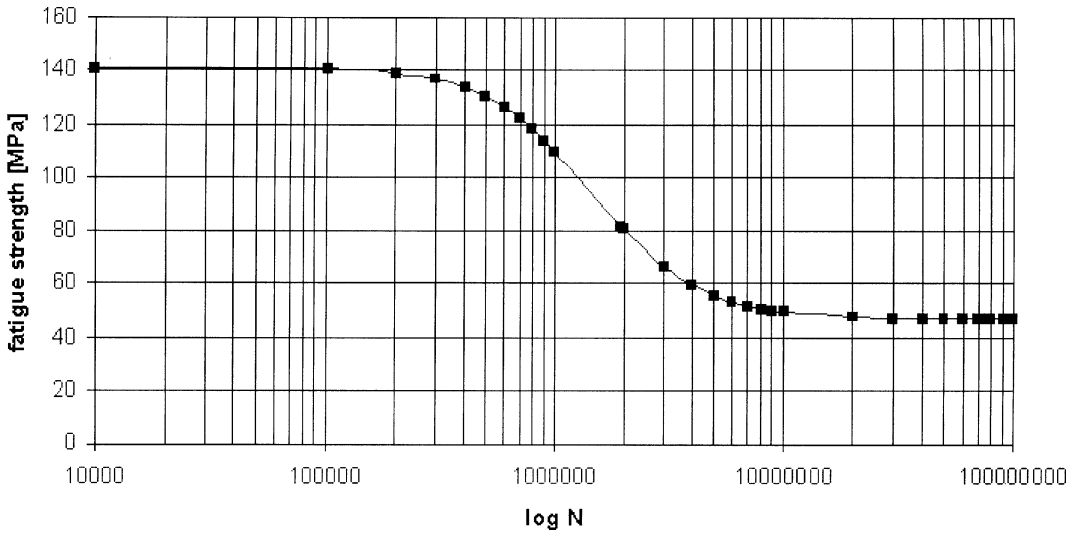

Fig. 15. Axial fatigue curve of testing bar.

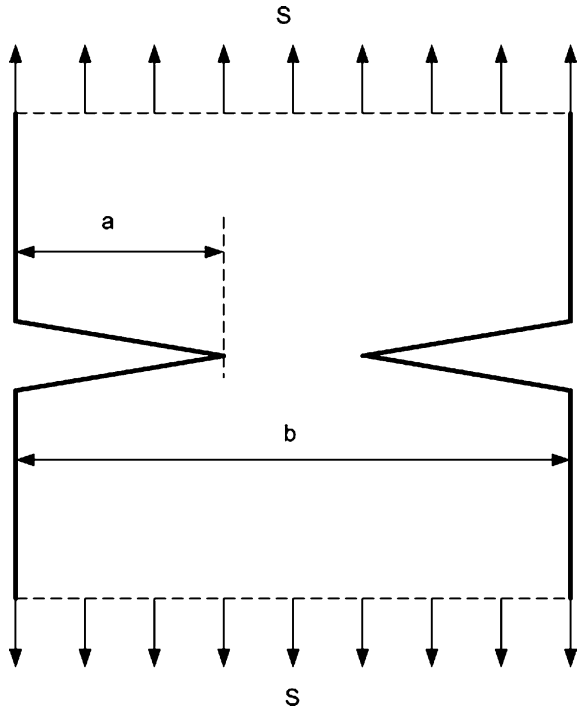

Fig. 16. External crack system of reinforced steel bar considered by Griffith's theory.

On the other hand the test values are approximately given in handbooks such as Ashby and Jones (1980): $G = 100\ \mathrm{kJ/m^2}$, $K = 140\ \mathrm{MN\,m^{-3/2}}$.

10. RDA fatigue crack propagation

10.1. Crack propagation of long bar with circular cross-section

The cracks may initiate early in service life (period from the fatigue life to the fatigue failure life) and propagate subcritically. The general approach to the analysis of the problem of the effect of maximum absolute stress in the cycle, $\sigma_{\max}$ on crack length must also be based on Bernoulli's energy theorem and localized reduction of cross-sectional area. Fatigue crack length as shown in Fig. 9 is

$$a = \frac{1}{2}\left(\phi_1 - \frac{\phi_1}{\sqrt[4]{\frac{2E_{\mathrm{H}}l_0^2}{\sigma_{\max}A^*\varphi^*}\frac{1}{1+\varphi^*}+1}}\right). \tag{102}$$

For cracks subjected to cyclically varying loads, maximum and minimum stress intensity factors, $K_{\max}$ and $K_{\min}$, defined at the extremes of the cycle, are assumed to prescribe crack growth. The stress range under cyclic loading is

$$\Delta\sigma = \sigma_{\max} - \sigma_{\min} = (1-r)\sigma_{\max}, \tag{103}$$

thus the RDA rate of release of potential energy range and stress intensity range are:

$$\Delta G_{\mathrm{I,c}} = \left(\frac{\phi_1}{\phi_{\mathrm{red}}} + 1\right)\frac{(1-r)^2\sigma_{\max}^2 l_0}{2E_{\mathrm{H}}}, \tag{104}$$

$$\Delta K_{\mathrm{I,c}} = \sqrt{\Delta G_{\mathrm{I,c}}E_{\mathrm{H}}}. \tag{105}$$

Crack growth and stress intensity range values are calculated by the RDA method (Table 3), on the above testing bar and finally presented in the form of log-log plots of a/N_{c} versus $\Delta K_{\mathrm{I,c}}$ (Fig. 17).

A $\sigma_{\max}$, maximum absolute stress in the cycle (42.50–268.50 MPa).

B $\frac{\phi_1}{\phi_{\mathrm{red}}} = \sqrt[4]{\frac{2E_{\mathrm{H}}l_0^2}{\sigma_{\max}A^*\varphi^*}\frac{1}{1+\varphi^*}+1}$, the ratio of initial diameter to the reduced diameter

C $a = \frac{1}{2}\left(\phi_1 - \frac{\phi_1}{\sqrt[4]{\frac{2E_{\mathrm{H}}l_0^2}{\sigma_{\max}A^*\varphi^*}\frac{1}{1+\varphi^*}+1}}\right)$, fatigue crack length

Table 3
Calculation of RDA fatigue crack growth a/N_{c}

A	B	C	D	E	F	G	H
42						49.8691603	IE-10
42.5	4.50739521	7.392353	2732.208777	3073350705	0.011842539	49.8691603	2.40531E–09
60	4.136121762	7.203162	1335.886124	1502684054	0.02201195	67.98904019	4.79353E–09
80	3.850190525	7.03259	720.7378823	810728776.4	0.036953833	88.09259243	8.6744E–09
100	3.642320574	6.891773	436.0121246	490452333.7	0.055265721	107.7302253	1.40519E–08
120	3.481017163	6.770913	281.346281	316475006.7	0.076817437	127.010479	2.13948E–08
140	3.350368959	6.664491	188.0876554	211572165.8	0.101508609	146.0027667	3.14998E–08
160	3.241288431	6.569067	127.5592206	143486187.4	0.129258314	164.7551091	4.57819E–08
180	3.148128412	6.482334	86.06112489	96806664.67	0.159999239	183.3025917	6.69617E–08
200	3.067155663	6.402668	56.37778116	63417076.67	0.193674079	201.6719034	1.00961E–07
220	2.99578236	6.328875	34.41546377	38712557.67	0.230233174	219.8839843	1.63484E-0-7
240	2.932146015	6.260052	17.71132025	19922744.94	0.26963287	237.9556736	3.14216E–07
260	2.874864654	6.195497	4.711568734	5299852.344	0.311834346	255.9007867	1.16899E–06
268.5	2.852177957	6.169212	0.045696183	51401.78067	0.330609734	263.492019	0.000120019

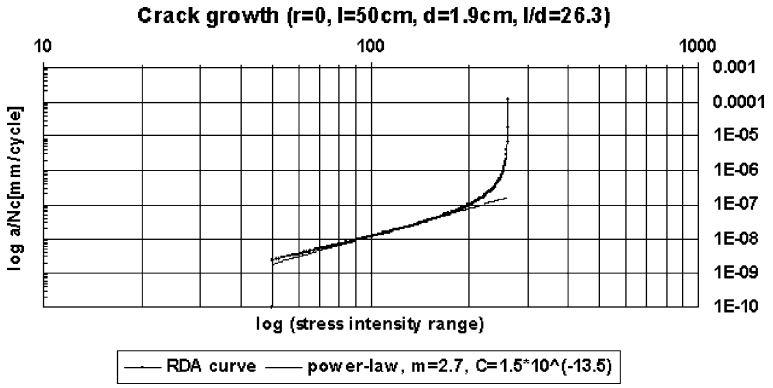

Fig. 17. Fatigue crack growth (a/N_c (mm/cycle)) as a function of stress intensity range ($\Delta K_{I,c}$ (MN(m$^{-3/2}$))) of testing bar ($l_0/\Phi = 26.3$).

D $\delta_c(-1) = \delta_e(-1)\left(-1 + \frac{G_{I,c}}{\frac{\sigma_{max}^2}{2E_H} l_0}\right)$, relative frequency for the fatigue failure life

E $N_c = \frac{\delta_c(-1)}{\delta_1}$, number of cycles for the fatigue failure life; $\delta_1 = 0.000000889$, relative frequency for the first cycle

F $\Delta G_{I,c} = \left(\frac{\phi_1}{\phi_{red}} + 1\right) \frac{(1-r)^2 \sigma_{max}^2 l_0}{2E_H}$, RDA rate of release of potential energy range

G $\Delta K_{I,c} = \sqrt{\Delta G_{I,c} E_H}$, RDA stress intensity range.

H $\frac{a}{N_c}$, RDA fatigue crack growth.

The sigmoidal variation of fatigue crack growth with $\Delta K_{I,c}$ is obtained from RDA calculation ($r = 0$) in terms of three regimes, as shown in Fig. 17. Curve in the second regime are compared to the best fit line of power-law (axis intercept, $C = 1.5 \times 10^{-13.5}$, slope of crack growth curve, $m = 2.7$).

This is evident from the fact that the crack growth relationship obtained here by RDA is very similar to the experimental crack propagation data.

The crack growth relationships most often used in engineering defect-tolerant design and lifetime calculations are based on mere empirical curves. Perhaps the safest approach to this problem has been to develop semiempirical relationships based on physical models for crack growth and then to determine the constants in the model by fitting to relevant experimental data.

10.2. Coefficient of asymmetry of cycle effect

The variation in the constant C with coefficient of asymmetry of cycle, r of above testing bar is shown in Fig. 18. At a given stress intensity range, crack growth or constant C increases with increasing coefficient of asymmetry of cycle. This effect named here as coefficient of asymmetry of cycle effect is known as load ratio effect. Similar behavior has been observed by Paris et al. (1972) in tests on A533B-1 steel specimens.

10.3. RDA fatigue size effect

Fatigue crack propagation data are generally measured using standard fracture mechanics-type specimen geometries, such as the compact tension, edge-notched bend, edge-notched tension, center-cracked sheet test-pieces, and so forth.

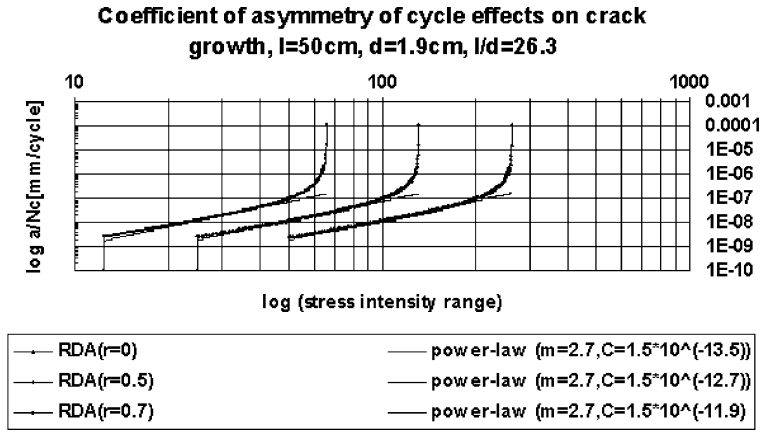

Fig. 18. Influence of coefficient of asymmetry of cycle on fatigue crack growth as a function of stress intensity range.

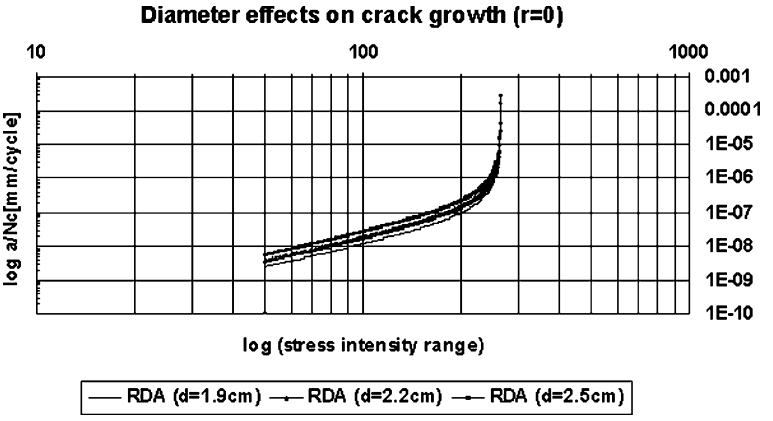

Fig. 19. Influence of diameter on fatigue crack growth as a function of stress intensity range.

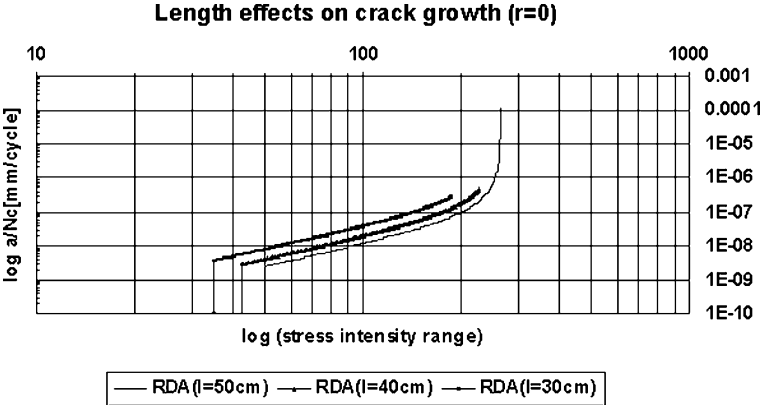

Fig. 20. Influence of length on fatigue crack growth as a function of stress intensity range.

In this section of the paper, the RDA modeling technique is used to investigate what is referred to here as the RDA fatigue size effect (see Figs. 19 and 20). The mechanical characteristics of testing bar are used in the calculation.

At a given stress intensity range, crack growth or constant C increases with increasing of diameter, but decreases with increasing of length of steel specimen. On the other hand, there is no changing of the slope of crack growth curve ($m = 2.7$).

11. Fatigue crack growth rate

According to the original analysis of Paris and his co-workers, the crack growth increment per cycle in fatigue ($\mathrm{d}a/\mathrm{d}N$) can be described in terms of a power law function of the range of K_{I}, given by the alternating stress intensity ($\Delta K = K_{\max} - K_{\min}$), thus:

$$\frac{\mathrm{d}a}{\mathrm{d}N} = C\Delta K^m, \tag{106}$$

where C and m are scaling constants for a particular material-heat-treatment condition. For structural steel: $C \sim 1.5 \times 10^{-11}, m \sim 2.75 - 3.0$. Test data are used to construct crack length versus number of cycles N plots, which are then differentiated, either graphically or numerically, to determine the rate of crack growth ($\mathrm{d}a/\mathrm{d}N$) for each crack length a_i.

First, to demonstrate the ability of the RDA analysis on fatigue crack growth rate, the axial fatigue setup of testing bar is used for results comparison obtained here by RDA modeling technique and a best fit line of Paris power-law (see Fig. 21).

The latter in order to demonstrate the effect of size on fatigue crack growth rate, the various sizes of reinforcing steel bars are analyzed and compared with a best fit lines of Paris power-law. The slope of crack growth rate curve, $\mathbf{m = 2.7}$ is not sufficiently different to be of interest, but axis intercept indicate fatigue size effect. Now, this fatigue size effect may be defined as the increase in constant C with decreasing of ratio l_0/ϕ of specimen. Specimen, $\phi = 2.5$ cm and $l_0/\phi = 5$ (see Fig. 22) have scaling constant, $\mathbf{C = 1.5 \times 10^{-10}}$ very similar to structural steel.

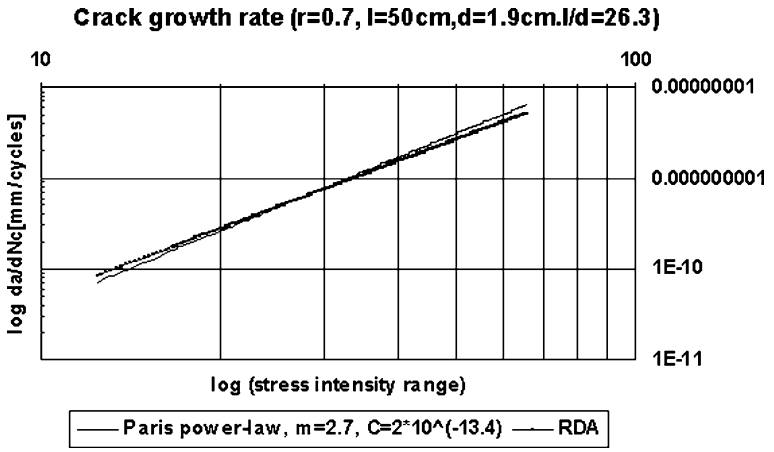

Fig. 21. Fatigue crack growth rate ($\mathrm{d}a/\mathrm{d}N_{\mathrm{c}}$ (mm/cycle)) as a function of stress intensity range ($\Delta K_{\mathrm{I,c}}$ (MN($\mathrm{m}^{-3/2}$))) of testing bar ($l_0/\Phi = 26.3$).

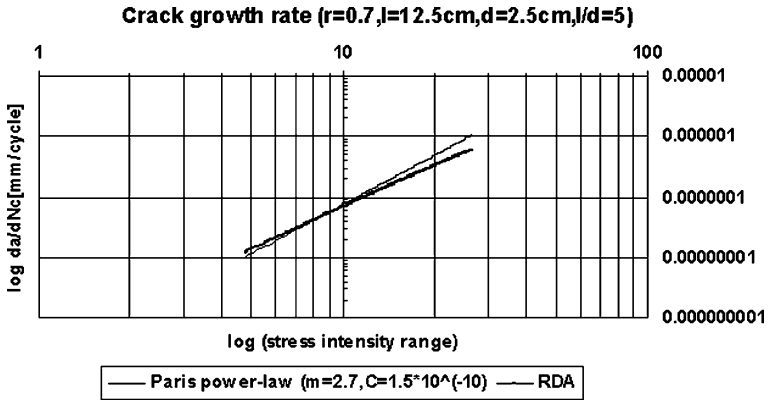

Fig. 22. Fatigue crack growth rate ($\mathrm{d}a/\mathrm{d}N_c$ (mm/cycle)) as a function of stress intensity range ($\Delta K_{I,c}$ (MN($m^{-3/2}$))) of smaller bar ($l_0/\Phi = 5$).

Let us examine a specimen with l_0/ϕ ratio of 5, which RDA results of fatigue growth rate are in good accordance with scaling constants of structural steel in terms of Paris power-law.

Slenderness ratio is 20 and the critical stress for it under quasi-static loading is yield sterss σ_Y (Milašinović, 2000). Then it can be easily established (Fig. 6., Haigh type diagram) that line determined under variable loading should be taken as the line of critical stresses.

$$\lim_{\delta\to\infty}\sigma_e(1) = \sigma_Y = 400 \text{ MPa},$$

$$\lim_{\delta\to\infty}\sigma_e(0) = \frac{1}{2}\left(1+\frac{1}{1+\varphi^*}\right)\sigma_Y = 267 \text{ MPa},$$

$$\lim_{\delta\to\infty}\sigma_e(-1) = \frac{1}{1+\varphi^*}\sigma_Y = 133 \text{ MPa}.$$

Now for this specimen the fatigue limit, $\sigma_e(-1)$ is in compliance with test results of axial fatigue of steel specimens ($\sigma_e(-1) \sim 0.28 \times \sigma_c = 0.28 \times 500 = 140$ MPa).

12. Conclusion

In the course of his research work, this author has developed a new model of viscoelasto-plastic material, which is able to describe the mutual interaction of elasticity, viscoelasticity and viscoplasticity. Based on this model, the RDA is established as the theoretical concept for studying the inelastic material deforming of materials and structures as well as to solve the dynamical problems. *By the RDA we involved one very complicate nonlinear viscoelasto-plastic problem into a simpler linear dynamical one.*

After examining the physical mechanism of the RDA on the base of energy transfer by mechanical wave motion, the subsequent sections give discussion of different special situations for the axial fatigue behavior in steel members. The main conclusions obtained are as follows:

(1) The theoretical value of the fatigue limit under constant stress amplitude is given by the following formula:

$$\sigma_e(r) = \frac{1}{2}\sigma_{max}\left[1+r+(1-r)\sqrt{\frac{(1+\varphi)^2+\delta^2}{1+\delta^2}}\frac{1}{1+\varphi}\right].$$

The proposed S–N curves are based on extensive theoretical studies using a newly proposed rheological model and RDA. Unlike previously available and purely empirical S–N curves, the newly developed S–N curves take into account the mechanical aspects of fatigue and cater for the influence of creep (creep coefficient) of material on the fatigue limit. However, comparison between the presently recommended design RDA S–N curves and those recommended by other methods, and previously available S–N curves are possible only for the same samples and experimental conditions.

(2) *Results of a new rheological model parameters obtained in the paper using Bernoulli's energy theorem identify an important relationship*, $\varphi^*(\mu)$ in rheology, which have not been considered before.

(3) *The theoretical value of the rate of release of viscoelastic energy obtained by RDA description of the hysteretic loop dissipation is given by the following formula*:

$$W_{\mathrm{d,ve}}(r) = \pi k \frac{1}{E_{\mathrm{H}}^2} \frac{(1-r)^2}{2} \sigma_{\max}^2 \frac{(1+\varphi^*)^2 + \delta^2}{1+\delta^2} \delta.$$

As a result, from the above formula and from the first law of thermodynamics we obtain: the relative frequency $\delta_{\mathrm{e}}(r)$ for theoretical estimation of the fatigue life, the change in the temperature of the body and the relative frequency $\delta_{\mathrm{c}}(r)$ for theoretical estimation of the fatigue failure life.

(4) The general approach to the analysis of the problem of fatigue failure is based on Bernoulli's energy theorem from which localized reduction of cross-section area is defined. Furthermore, the RDA fracture stress σ_{c} and the maximum applied dynamical stress $\sigma_{\max,\mathrm{c}}$ are obtained.

(5) *The RDA rate of release of potential energy*, $G_{I,c}$ *has been analyzed under the hypothesis that in period from the fatigue life to the fatigue failure life the reduction of the cross-section area goes on*. In the case of axial loading of long bar with circular cross-section it is expressed by the following formula

$$G_{\mathrm{I,c}} = \left(\sqrt[4]{\frac{2E_{\mathrm{H}} l_0^2}{\sigma_{\max,\mathrm{c}} A^* \varphi^*} \frac{1}{1+\varphi^*} + 1} + 1 \right) \frac{\sigma_{\max,\mathrm{c}}^2 l_0}{2E_{\mathrm{H}}}.$$

Two various methods of determining the rate of release of potential energy G_{I} have been compared. The emphasis has been to show that RDA method enables the rate of release of potential energy to be calculated from this theory, differently obtained by Griffith's theory, or experimentally. On the basis of the comparisons, the present method is regarded as valid and suitable (RDA: $G_{\mathrm{I,c}} = 85.88$ kJ/m^2, $K_{\mathrm{I,c}} = 134.294$ MN m$^{-3/2}$; Griffith: $G_{\mathrm{I}} = 88.368$ kJ/m^2, $K_{\mathrm{I}} = 136.225$ MN m$^{-3/2}$).

(6) Axial fatigue experiment of reinforcing steel bar was performed. *After the experimental investigations it may be concluded that the presented RDA method is well confirmed by the temperature measurements.*

(7) The sigmoidal variation of fatigue crack propagation with $\Delta K_{\mathrm{I,c}}$ is obtained from RDA calculation in terms of three regimes. Curve in the second regime is compared to a best fit line of power-law. *This is evident from the fact that the crack propagation relationship obtained here by RDA is very similar to the experimental crack propagation data.*

At a given stress intensity range, crack growth or constant C increases with an increase of coefficient of asymmetry of cycle. This effect named here as coefficient of asymmetry of cycle effect is known as load ratio effect.

The RDA modeling technique is used to investigate the effect of size on fatigue crack growth. At a given stress intensity range, crack growth or constant C increases with an increase of diameter, but decreasing with an increase of length of steel specimen. On the other hand, there is no changing to the slope of crack growth curve, $m = 2.7$. This is referred here as the RDA fatigue size effect.

(8) The ability of the RDA analysis on fatigue crack growth rate is demonstrated. The axial fatigue setup of testing bar is used for results comparison obtained here by RDA modeling technique and a best fit line of Paris power-law.

To demonstrate the effect of size on fatigue crack rate, the various sizes of reinforcing steel bars are analyzed and compared with a best fit lines of Paris power-law. The slope of crack growth rate curve, $m = 2.7$ is not sufficiently different to be of interest, but axis intercept, C indicate fatigue size effect. This effect of size on fatigue crack growth rate is defined here as the increase in constant C with decreasing of ratio l_0/ϕ of specimen.

Due to the present observation, fundamentally new, our understanding of fatigue may be achieved. The analytical RDA method is valid and suitable for modeling of fatigue behavior.

References

Ashby, M.F., Jones, D.H.R., 1980. Engineering Materials, An Introduction to their Properties and Applications. Pergamon Press, London.

Dugdale, D.S., 1960. Yielding of steel sheets containing slits. J. Mech. Phys. Solids 8, 100–104.

Dowling, N.E., 1976. In: Cracks and Fracture, ASTM STP 601. American Society for Testing and Materials, Philadelphia, Pensylvania, p. 19.

Griffith, A.A., 1921. The phenomena of rupture and flow in solids. Philos. Trans. Roy. Soc. London, Ser. A. 221, 163–198.

Griffith, A.A., 1925. in: C.B. Biezeno, J.M. Burgers (Eds.), Proc. 1st Int. Conf. Appl. Mech. Delft, Technische Boekhandel en Drukkerij, vol. 55.

Hillerborg, A., Modeer, M., Petersson, P.E., 1976. Cem. Concr. Res. 6, 773.

Inglish, C.E., 1913. Stresses in a plate due to the presence of cracks and sharp corners. Trans. Inst. Naval Archit. 55, 219–230.

Irwin, G.R., 1948. Fracturing of Metals. Proc. ASM Symp., Chicago, Cleveland, p. 147–166.

Kojić, M., 1997. Computational procedures in inelastic analysis of solids and structures. Center for Scientific Research of Serbian Academy of Sciences and Arts and University of Kragujevac, Yu.

Lubarda, V.A., Šumarac, D., Krajčinovič, D., 1992. Hysteretic response of ductile materials subjected to cycling loads. in: JU, J.W. (Ed.), Recent Advances in Damage Mechanics and Plasticity, vol. 145-157. ASME Publication, AMD-vol. 132, New York.

Milašinović, D.D., 1996. Rheological–dynamical analogy. Scientific Meetings of the Serbian Academy of Sciences and Arts, Department of Technical Sciences, Reprint (in Serbian), vol. LXXXIII, Book 2, Belgrade, YU, p. 103–110.

Milašinović, D.D., 1997. The Finite Strip Method in Computational Mechanics. Faculties of Civil Engineering: Subotica, Budapest, Belgrade, p. 416.

Milašinović, D.D., 2000. Rheological–dynamical analogy: prediction of buckling curves of columns. Int. J. Solids Struct. 37, 3965–4004.

Orowan, E., 1948. Rept. Prog. Phys. 12, 185.

Paris, P.C., Gomez, M.P., Anderson, W.E., 1961. Rational analytic theory of fatigue. The Trend in Engineering 13, 9–14.

Paris, P.C., Erdogan, F., 1963. A critical analysis of crack propagation laws. Trans. ASME (Series D) 85, 528–534.

Paris, P.C. et al., 1972. Extensive study of low fatigue crack growth rates in A533 and A508 Steels. Proc. 1971 Symp. On Fractyre Mech., Part I, ASTM STP 513, American Society for Testing and Materials, Philadelphia, PA, p. 141–176.

Reiner, M., 1955. Rhe'ologie the'orique. Dunod, Paris, France.

Rice, J.R., Rosengren, G.F., 1968. Plane strain deformation near crack tip in a power-law hardening material. J. Mech. Phys. Solids 16, 1–12.

Rooke, D.P., Cartwright, D.J., 1976. Compendium of Stress Intensity Factors. H.M. Stationery Office, London.

Tada, H., Paris, P.C., Irwin, G.R., 1973. The Stress Analysis of Cracks Handbook. Del Research Corporation, Hellertown, Pennsylvania.

Timoshenko, S.P., Goodier, J.N., 1951. Theory of Elasticity. McGraw-Hill, New York.

Wells, A.A., 1961. Unstable crack propagation in metals, cleavage and fast fracture. In: Proc. Crack Propagation Sym., vol. 1. College of Aeronautics, Cranfield, pp. 210–230.

Wöhler, M., 1867. Wöhler's experiments on the strength of metals. Engineering, August 23.